



First rare earth ions doped Si based down converter layers integration in an industrial Si solar cell

J. Cardin¹, L. Dumont¹, C. Labbé¹, P.-M. Anglade¹, M. Vallet², M. Carrada², S.C. Wu³, I.-S. Yu³, A. L. Richard⁴, W. M. Jadwisienczak⁴, X. Portier¹, P. Marie¹, F. Gourbilleau¹

¹ CIMAP, Normandie Univ, ENSICAEN, UNICAEN, CEA, CNRS, 6 Boulevard Maréchal Juin 14050 Caen Cedex 4, France

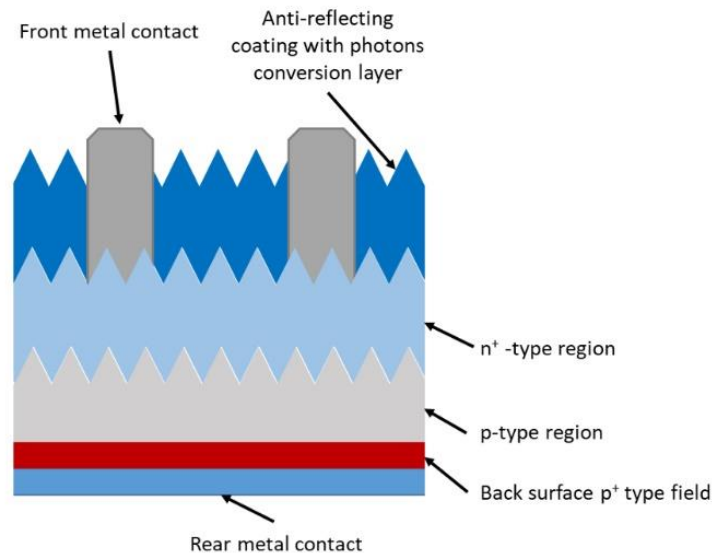
² CEMES-CNRS, Université de Toulouse, 29 rue J. Marvig, 31055 Toulouse Cedex 04, France

³ Department of Materials Science and Engineering, National Dong Hwa University, Hualien, Taiwan

⁴ Ohio University, Athens, OH 45701, USA

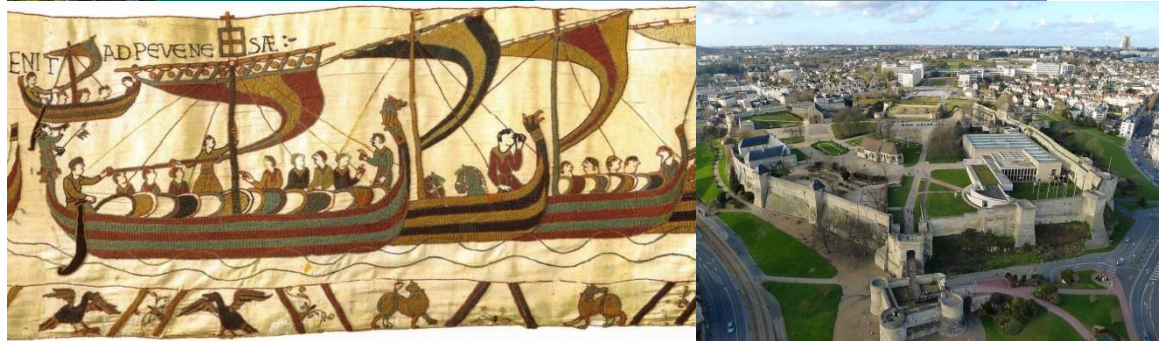
Outline

- Introduction
- Growth of thin films by RF magnetron sputtering
- Frequency layer optimization
- Modeling of Donor (Tb^{3+})-Acceptor(Yb^{3+}) ions system
- Integration in an industrial process
- Conclusion



Introduction

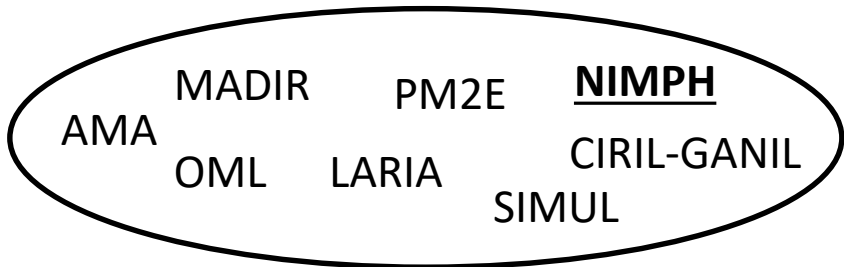
CIMAP Lab



In Caen, Normandie (2h with car in the west from Paris)

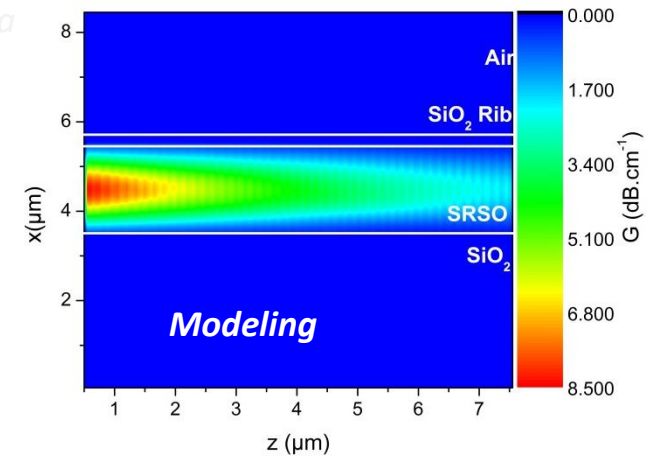
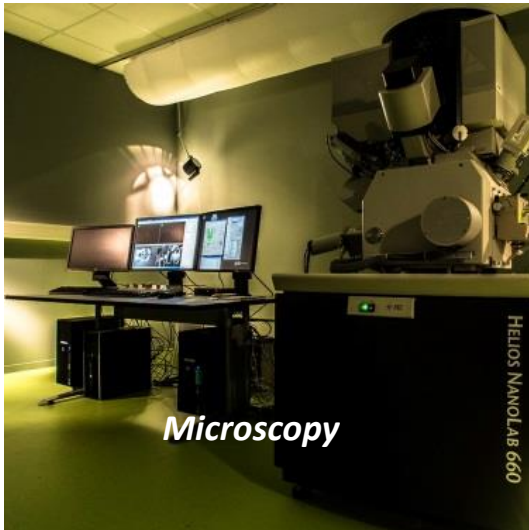


University of Caen Normandie, Ensicaen, CNRS, CEA

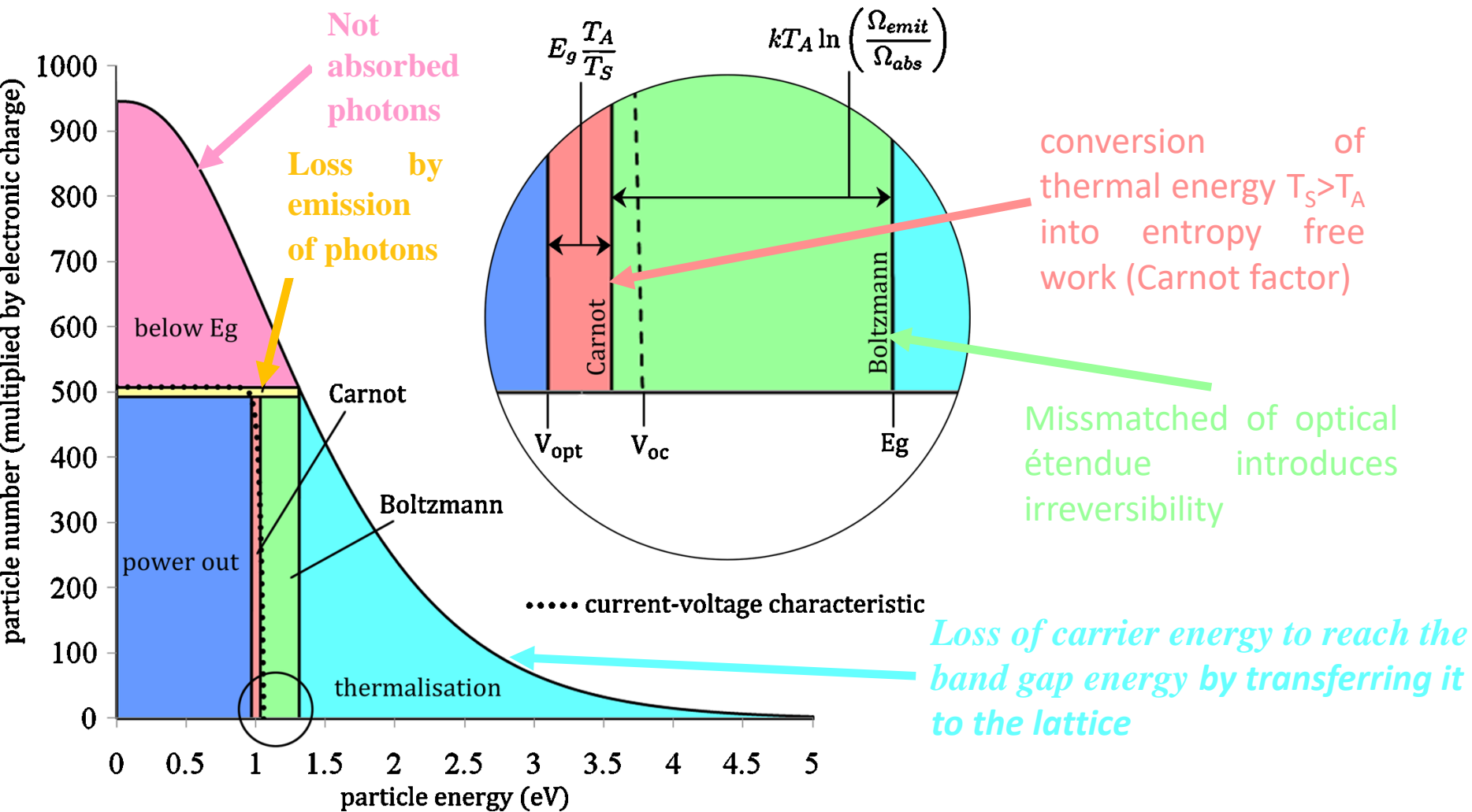


7 teams with various activities : irradiation with heavy ions, optical materials for laser and photonics, material for energy, defects studies in SC + biosourced materials...+ **CIRIL platform leading the researches** at the GANIL facility

NIMPH Team

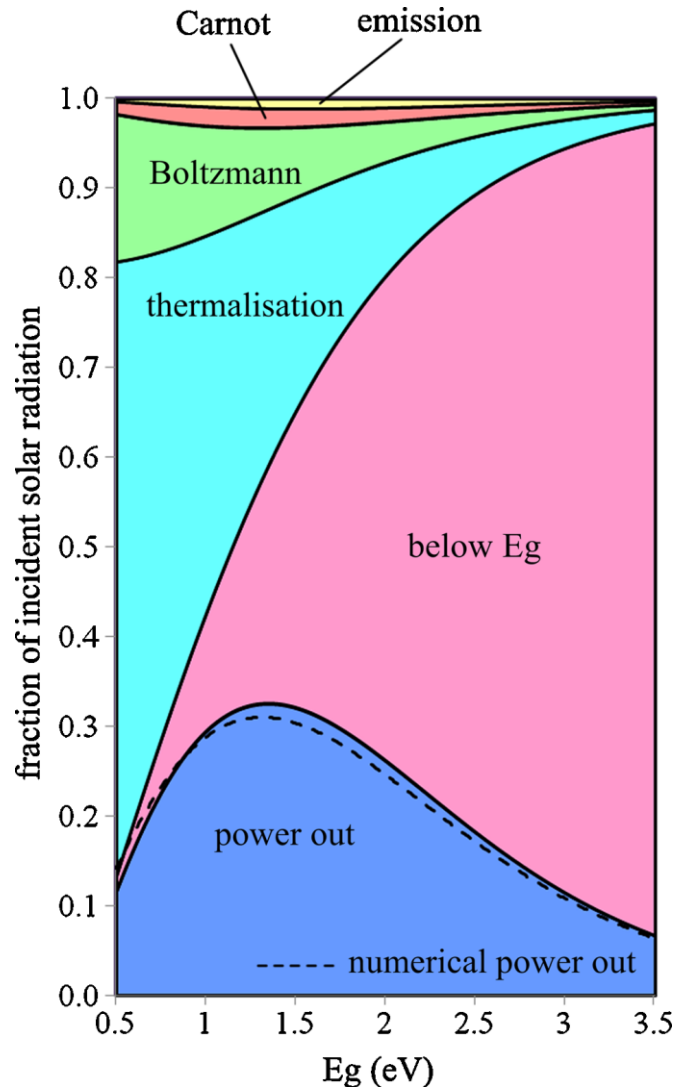


Losses in solar cells



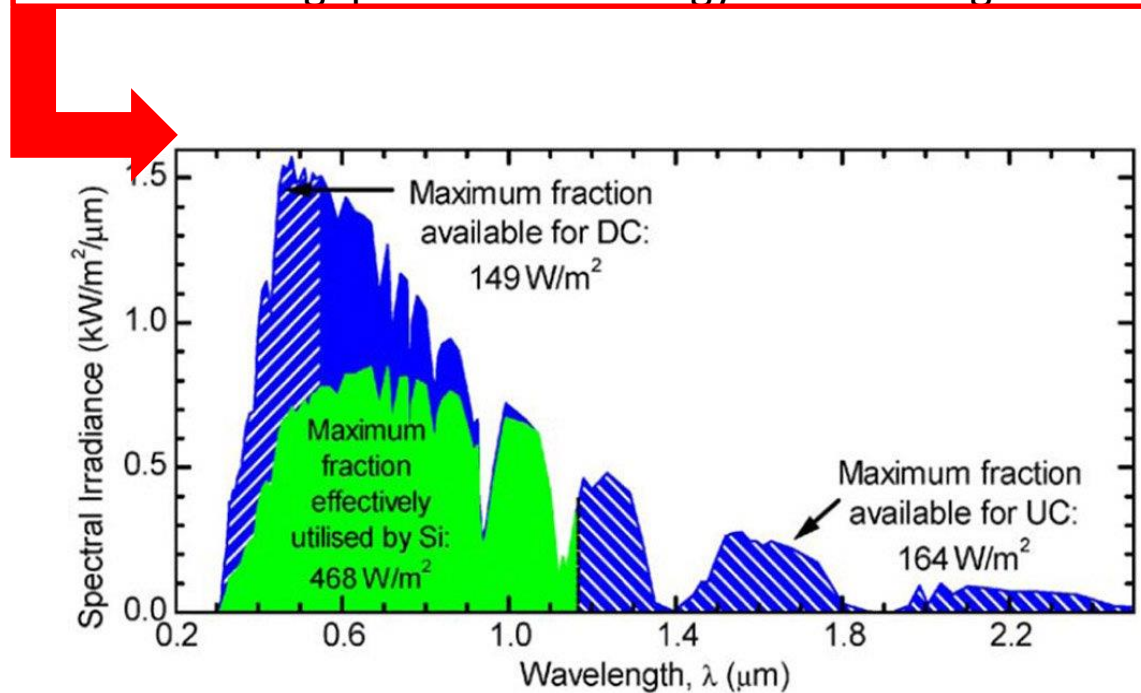
Fundamental losses in solar cells, Prog. Photovolt: Res. Appl., LC Hirst, N J Ekins-Daukes, 19:286-293, 2011

Losses in Solar Cells : limited efficiency



Different kind of losses:

- Emission : recombination of carrier \rightarrow PL
- Carnot limit : unavoidable heat loss to the surroundings
- Boltzmann : irreversible entropy generation
- Thermalization : carrier with energy largely above SC E_g
- Below SC E_g : photon with energy below SC E_g

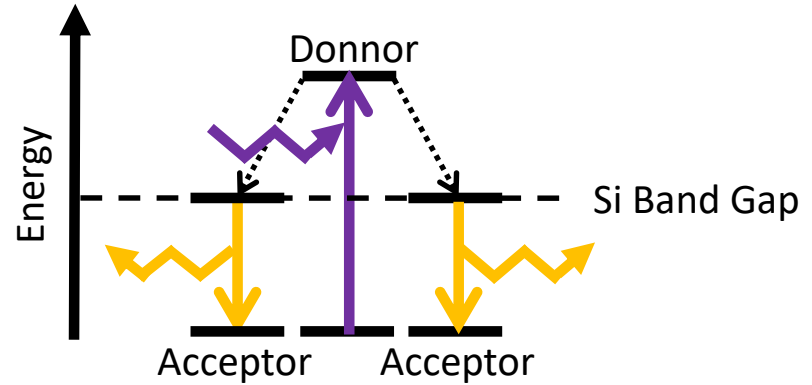
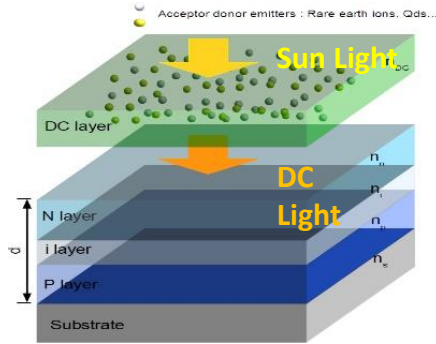


Fundamental losses in solar cells, Prog. Photovolt: Res. Appl., LC Hirst, N J Ekins-Daukes, 19:286–293, 2011

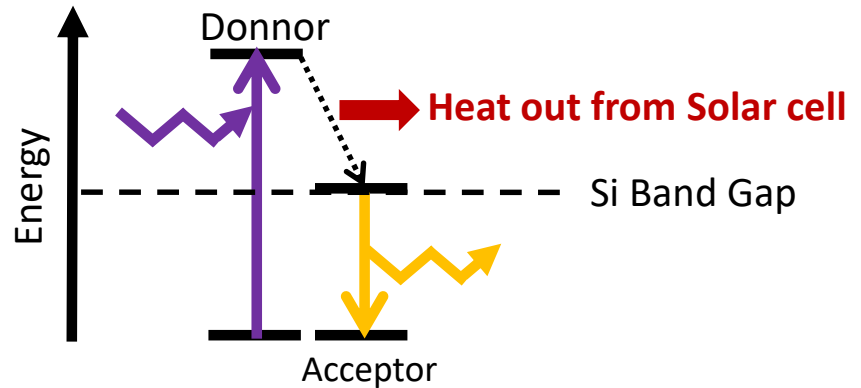
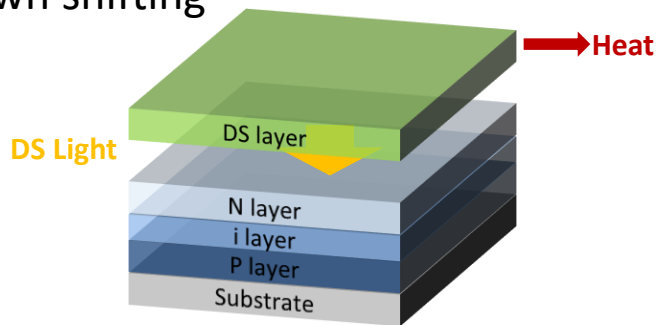
Yao Zhu et al, 7 January 2013, SPIE Newsroom. DOI: 10.1117/2.1201212.004585

Solar irradiance conversion with solar cell

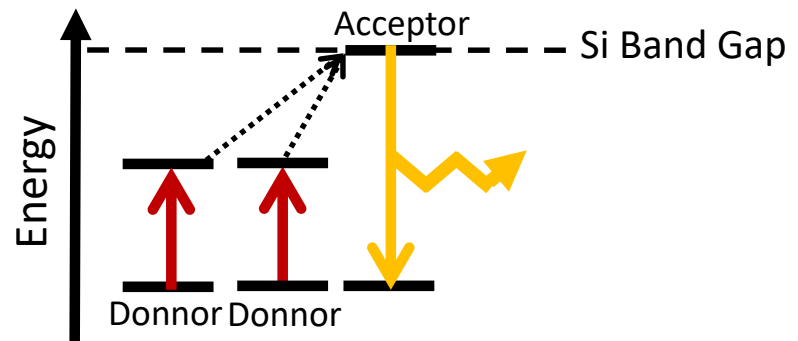
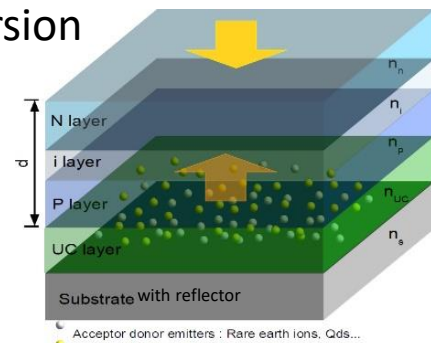
Down conversion



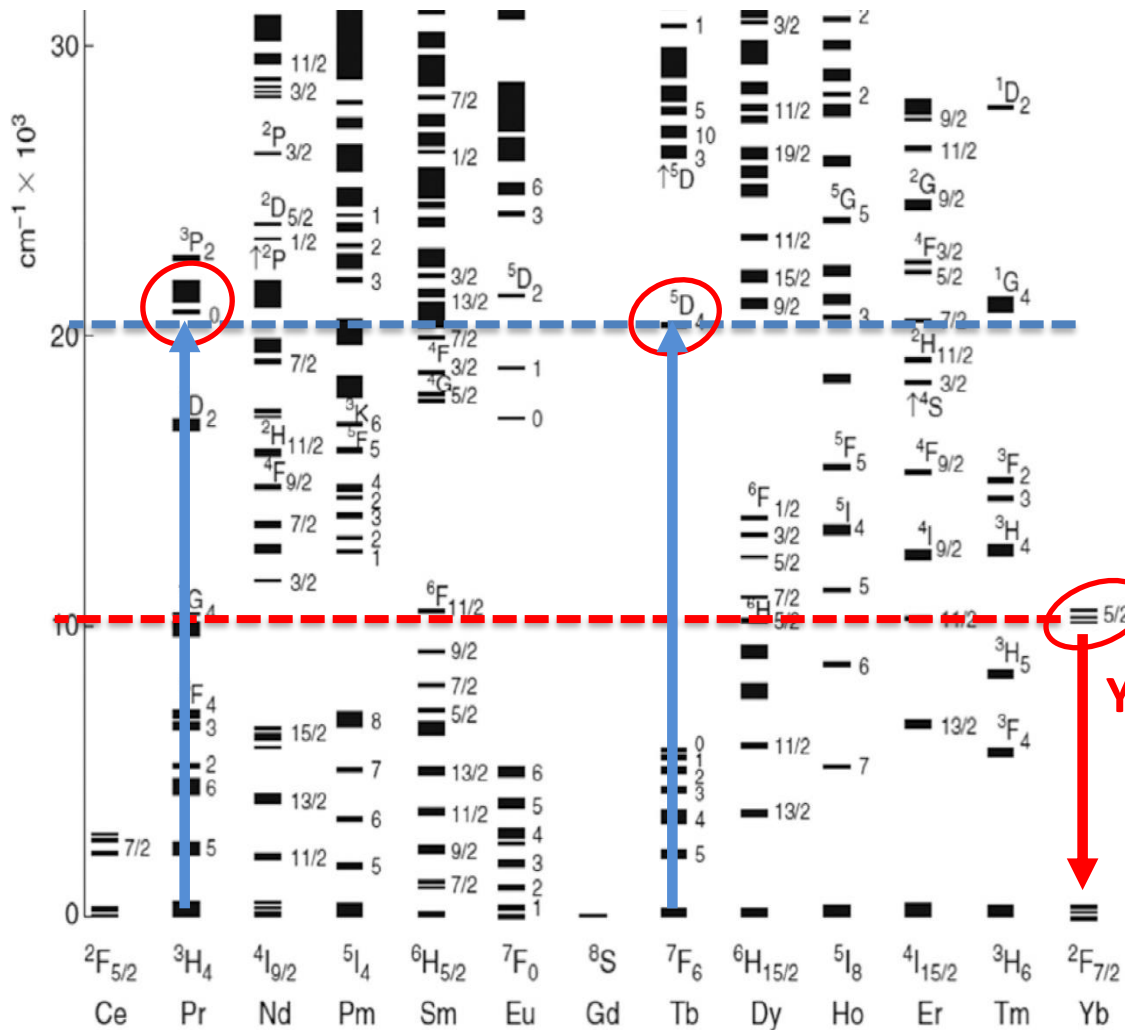
Down shifting



Up conversion



Rare earth ions for donor-acceptor system



Pr³⁺, Tb³⁺

Absorption at about 500nm (2,48eV)
 -> twice the SC BG

Yb³⁺

Emission at about 1000nm (1,24eV)
 -> once the SC BG

G. H. Dieke and H. M. Crosswhite, *Applied Optics* Vol. 2, Issue 7, pp. 675-686 (1963)

Development of frequency conversion layer

ADVANCED OPTICAL MATERIALS
Explore this journal >

Full Paper

Highly Efficient Infrared Quantum Cutting in Tb³⁺-Yb³⁺ Codoped Silicon Oxynitride for Solar Cell Applications

Yong-Tao An, Christophe Labbé, Julien Cardin, Magali Morales, Fabrice Gourbilleau

First published: 10 September 2013 Full publication history

DOI: 10.1002/adom.201300186 View/save citation

Si_xO_y:Tb³⁺:Yb³⁺ efficient QC for frequency conversion layer

2013

PhD YT An



PhD L Dumont

2017 Si_x:Tb³⁺:Yb³⁺ efficient DS layer

Solar Energy Materials and Solar Cells
Volume 169, September 2017, Pages 132-144

Down-shifting Si-based layer for Si solar applications

L. Dumont^a, P. Benzo^{a, 1}, J. Cardin^a, I.-S. Yu^b, C. Labbé^a, P. Marie^a, C. Dufour^a, G. Zatyrb^c, A. Podhorodecki^c, F. Gourbilleau^{a, 2}

2016

Solar Energy Materials and Solar Cells
Volume 145, Part 2, February 2016, Pages 84-92

Si_x:Tb³⁺-Yb³⁺, an efficient down-conversion layer compatible with a silicon solar cell process

Lucile Dumont^{a, 2}, Julien Cardin^{a, 2}, Patrizio Benzo^{a, 1, 2}, Marzia Carrada^{b, 2}, Christophe Labbé^{a, 2}, Andrea L. Richard^{c, 2}, David C. Ingram^{c, 2}, Wojciech M. Jadwisnienczak^{d, 2}, Fabrice Gourbilleau^{a, 2}

2016 Si_x:Tb³⁺:Yb³⁺ efficient DC layer

2017

Journal of Rare Earths
Available online 7 November 2018
In Press, Accepted Manuscript

Monolithic crystalline silicon solar cells with Si_x layers doped with Tb³⁺ and Yb³⁺ rare-earth ions

Ing-Song Yu^{a, 2}, Shao-Chun Wu^a, Lucile Dumont^b, Julien Cardin^b, Christophe Labbé^b, Fabrice Gourbilleau^b

Show more

https://doi.org/10.1016/j.jre.2018.07.014

Si_x:Tb³⁺:Yb³⁺ based efficient DC layer topped on SI solar cell with an relative increase by 1.34% in the conversion efficiency

Received: 13 April 2018 | Revised: 6 July 2018 | Accepted: 30 July 2018
DOI: 10.1002/pip.3071

RESEARCH ARTICLE

WILEY PHOTOVOLTAICS

First down converter multilayers integration in an industrial Si solar cell process

Lucile Dumont¹ | Julien Cardin¹ | Christophe Labbé¹ | Cédric Frilay¹ | Pierre-Matthieu Anglade¹ | Ing-Song Yu² | Maxime Vallet³ | Patrick Benzo³ | Marzia Carrada² | Didier Stiévenard⁴ | Hocine Merabet⁵ | Fabrice Gourbilleau¹

Si_x:Tb³⁺:Yb³⁺ efficient Multilayer DC layer topped on Si solar cell.

2019

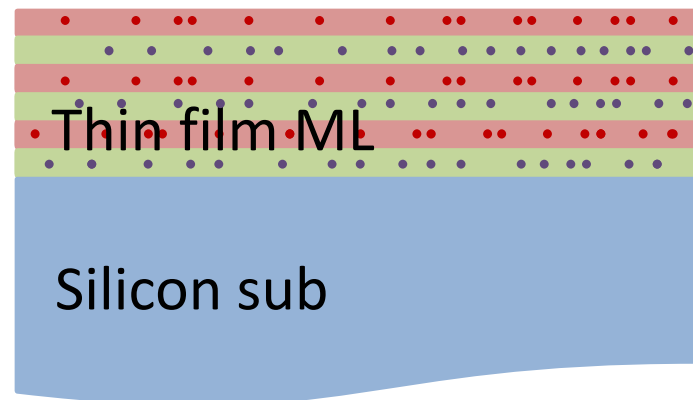
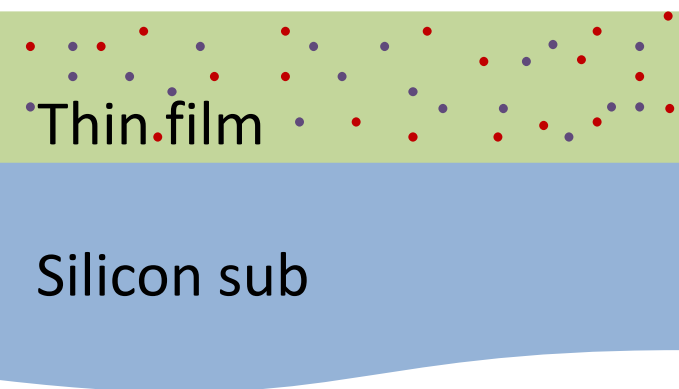
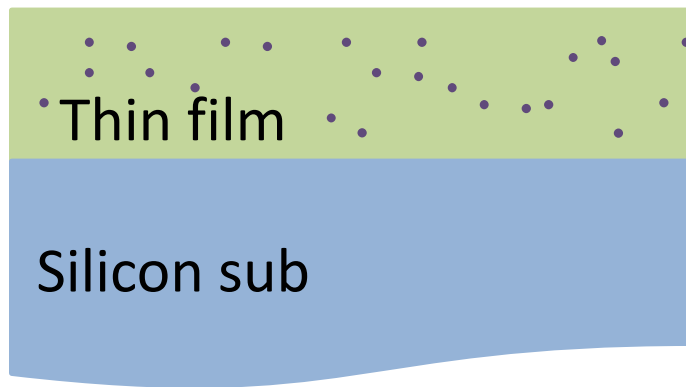
Growth of thin films by RF magnetron sputtering

Important parameters

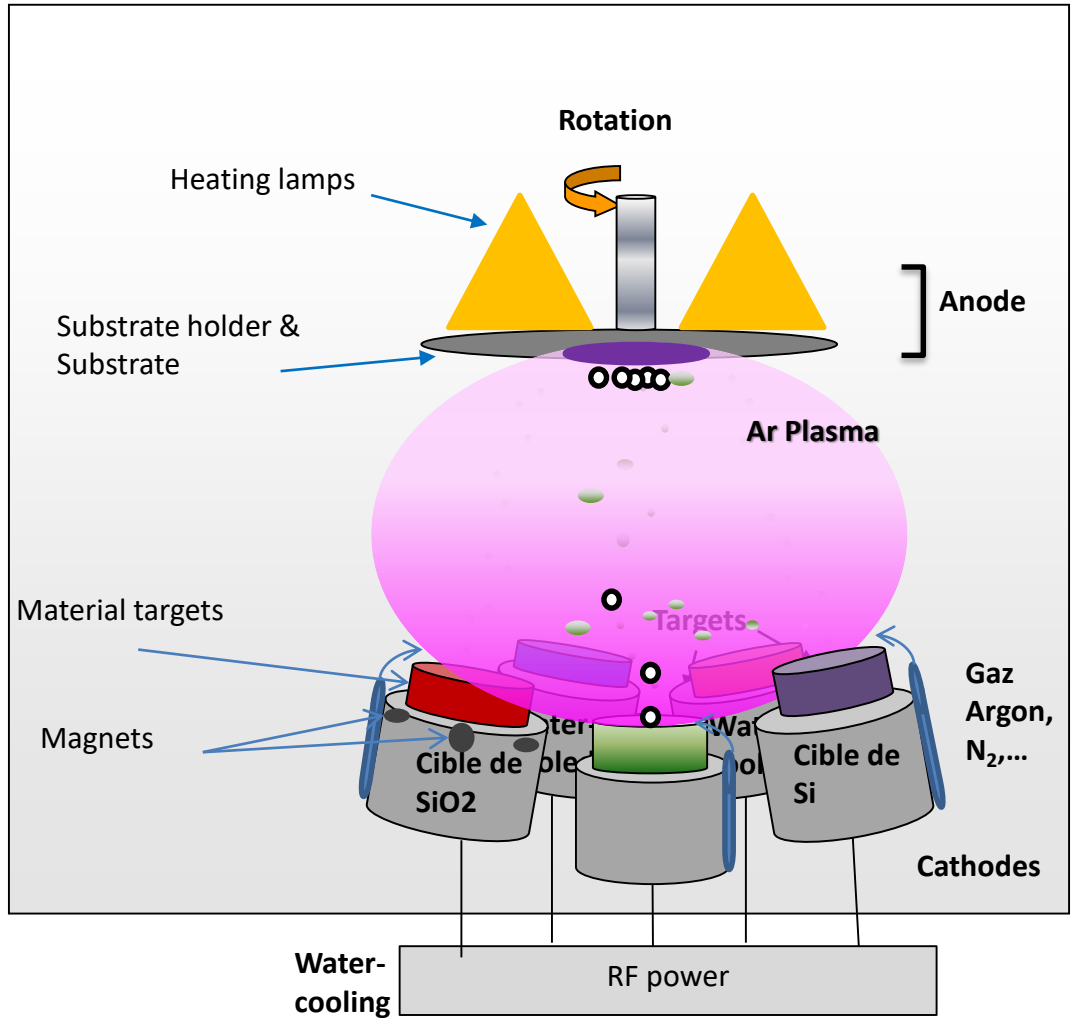
- **Chemical :**
 - rare earth (RE) ratio
 - activation of rare earth(RE^{3+})
 - high concentration required
- **Physical :**
 - energy matching between host matrix density of states and RE states
 - RE low excitation cross-section (10^{-21} cm^2)
 - Cross relaxation between same kind of RE
 - Excitation of Donor ions directly or indirectly (matrix sensitization)->Matrix (SiO_x , SiN_x , SiO_xN_y) properties
 - Cooperative energy transfer from donor (D) to acceptor (A) ion->D-A distance dependent
 - Relaxation mechanisms through energy transfer between the same kind of ions->distance dependent
- **Optical :**
 - transparent in 550-1200nm range and efficient in UV (DC) or in IR (UC)
- **Technological Process :**
 - Compatible with Si solar cell process
 - stable in time (20-25years), non toxic

Si based down shifting and down conversion layers in homogenous and multi layer configurations

- SiO_y
 - SiN_xO_y
 - SiN_x
- } : $\text{Tb}^{3+}\text{Yb}^{3+}$

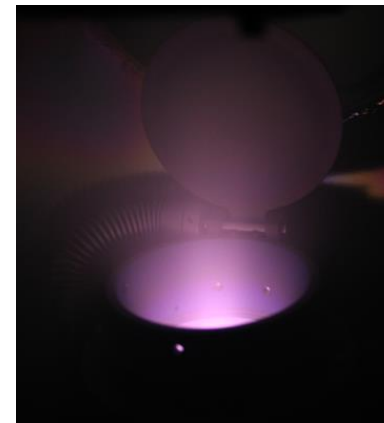


Growth of thin films by RF magnetron sputtering



Grown of thin film by magnetron sputtering

- Depositions parameters:
- Deposition Temperature , T_{dp} ($^{\circ}C$)
- Plasma Pressure, P_{tot} (sccm)
- Gaz : Argon and nitrogen
 - Nitrogen rate, rN_2
- RF Power density on target, P_{target} (W/cm^2)
- Depositing time, t_{dp} (s)

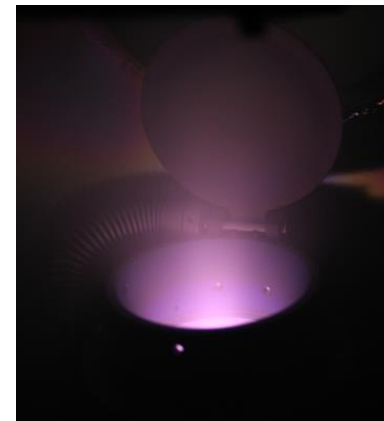


*Confocales
targets conf.*

Plasma

Grown of thin film by magnetron sputtering

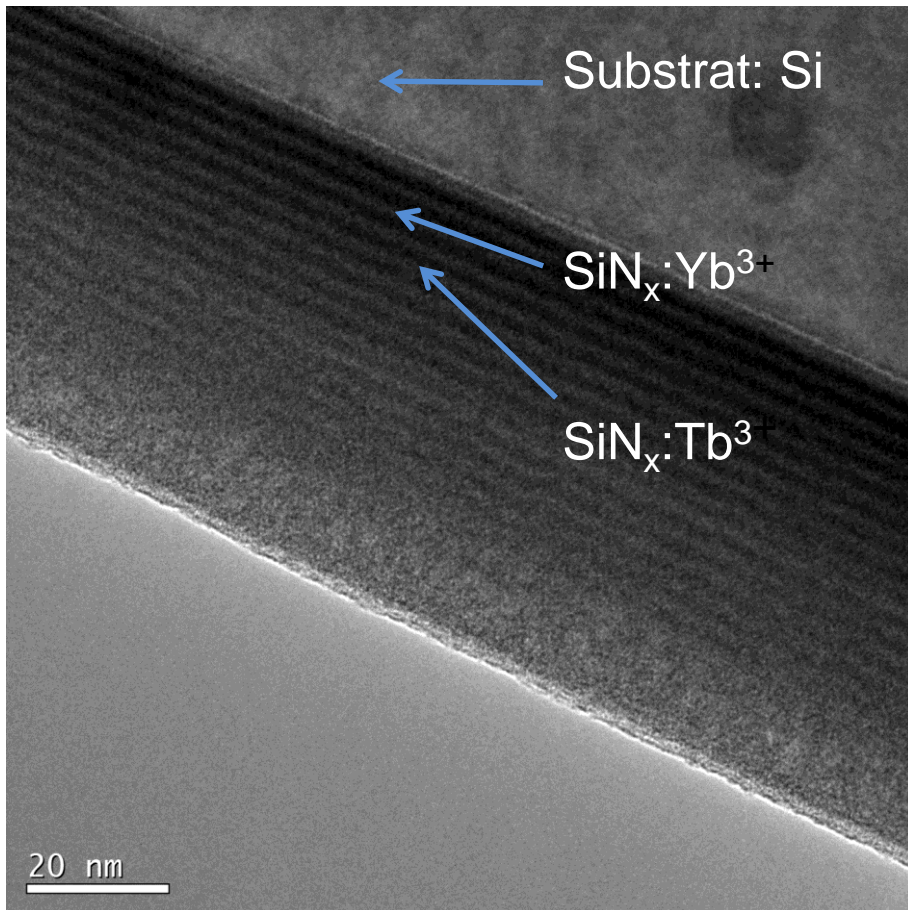
- Depositions parameters:
- Deposition Temperature , T_{dp} ($^{\circ}\text{C}$)
- Plasma Pressure, P_{tot} (sccm)
- Gaz : Argon and nitrogen
 - Nitrogen rate, rN_2
- RF Power density on target, P_{target} (W/cm^2)
- Depositing time, t_{dp} (s)
- **Annealing with rapid or slow ramp of T under specific gas (N_2 , Forming...)**



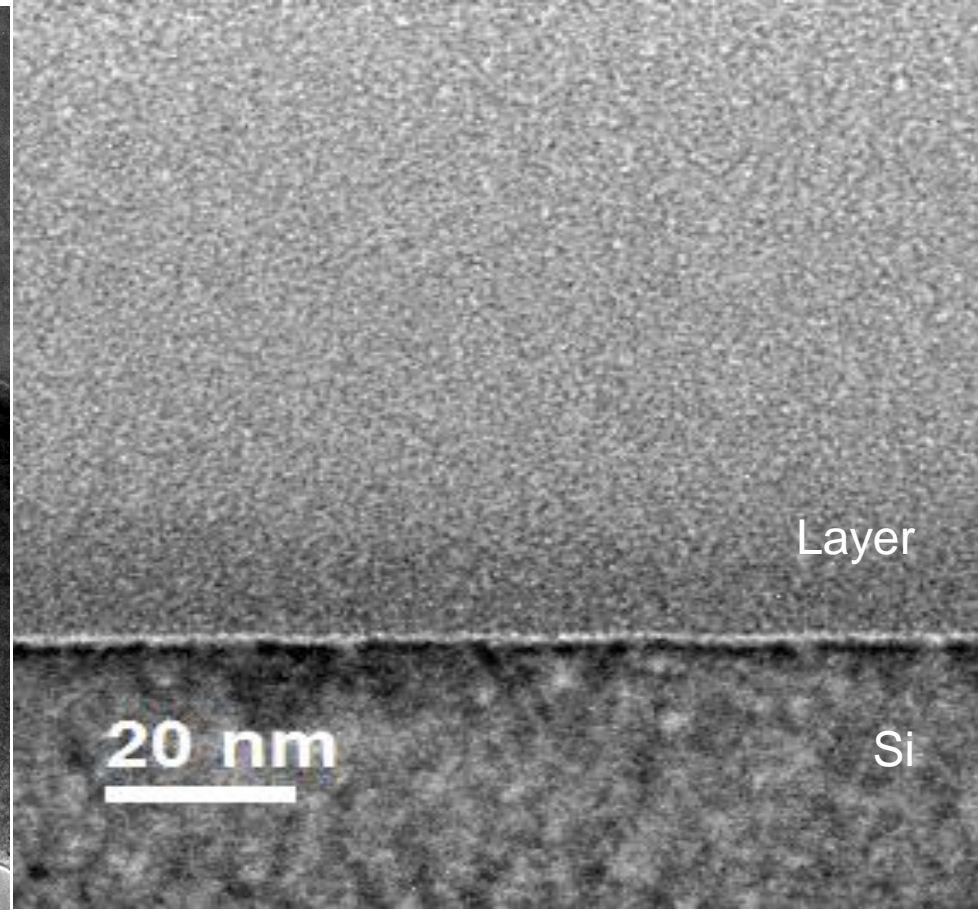
*Confocales
targets conf.*

Plasma

Homogenous thin film and multilayer systems

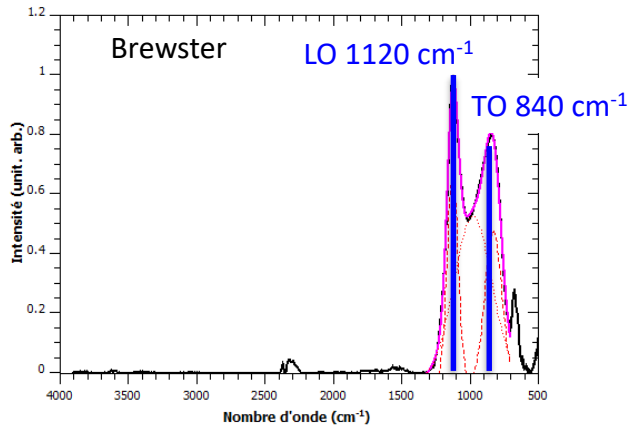


Cross-section view of the optimized multilayer system.

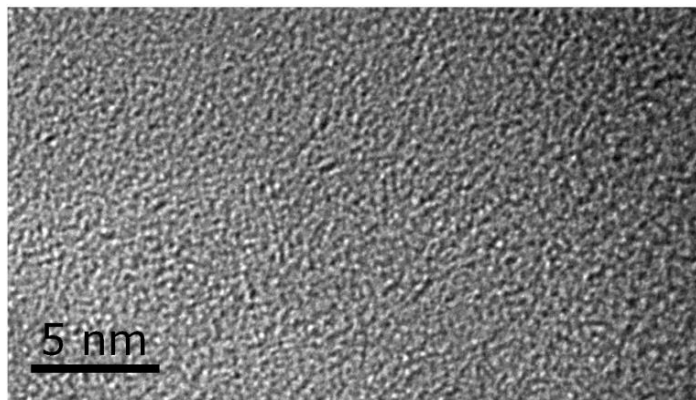


Cross-section view of the optimized homogenous layer system

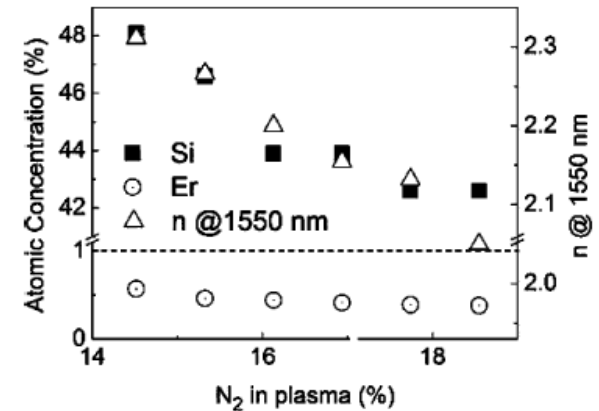
Structural and physical properties of Si based layer grown by magnetron sputtering



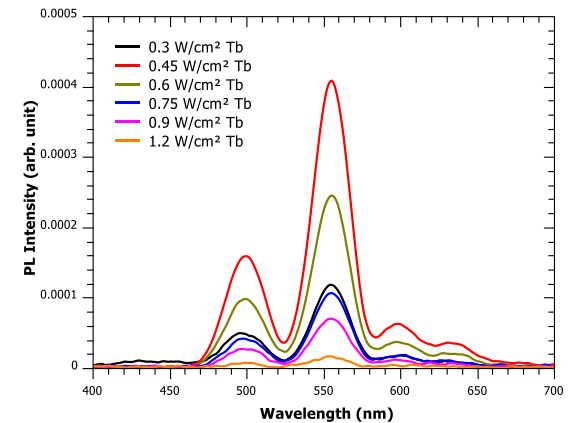
Control of the stoichiometry by tuning the sputtering parameters: SiN_x [FTIR]



Amorphous and homogenous films: SiN_x [HRTEM]



Control of refractive index by tuning the sputtering parameters : SiN_x [ELLIPSOMETRY]



Si based doped with rare earth ions luminescent layer: $\text{SiN}_x\text{-Tb}^{3+}$ [PHOTOLUMINESCENCE]

Frequency layer optimization

Down conversion layer



[Explore this journal](#)

Full Paper

Highly Efficient Infrared Quantum Cutting in Tb^{3+} - Yb^{3+} Codoped Silicon Oxynitride for Solar Cell Applications

Yong-Tao An, Christophe Labbé, Julien Cardin, Magali Morales, Fabrice Gourbilleau

First published: 10 September 2013 [Full publication history](#)

DOI: 10.1002/adom.201300186 [View/save citation](#)



Solar Energy Materials and Solar Cells

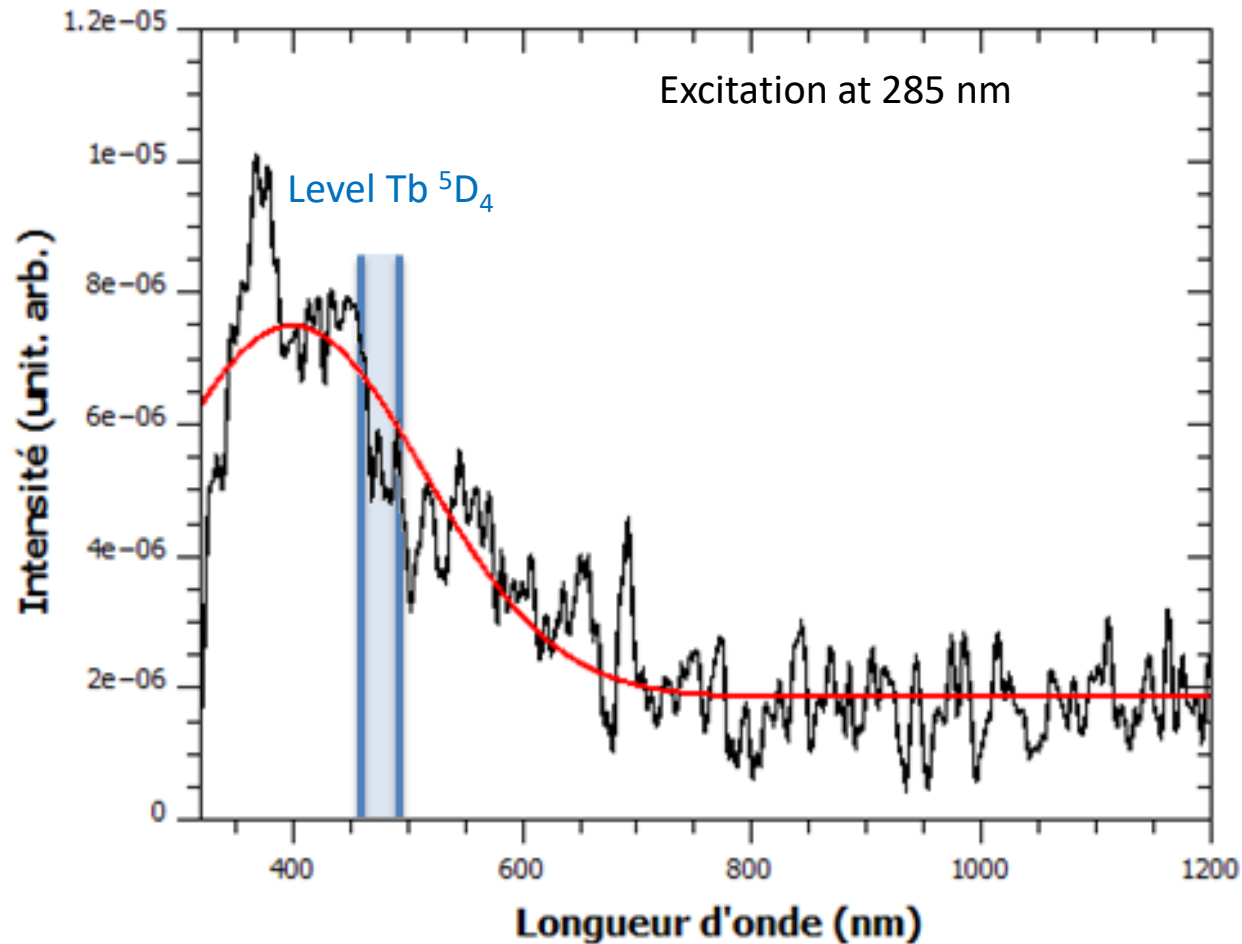
Volume 145, Part 2, February 2016, Pages 84-92



$SiN_x:Tb^{3+}-Yb^{3+}$, an efficient down-conversion layer compatible with a silicon solar cell process

Lucile Dumont ^{a, b, c}, Julien Cardin ^{a, b, c}, Patrizio Benzo ^{a, 1, b, c}, Marzia Carrada ^{b, c}, Christophe Labbé ^{a, b, c}, Andrea L. Richard ^{c, d, e}, David C. Ingram ^{c, d, e}, Wojciech M. Jadwisieniczak ^{d, e}, Fabrice Gourbilleau ^{a, b, c}

SiN_x matrix photoluminescence

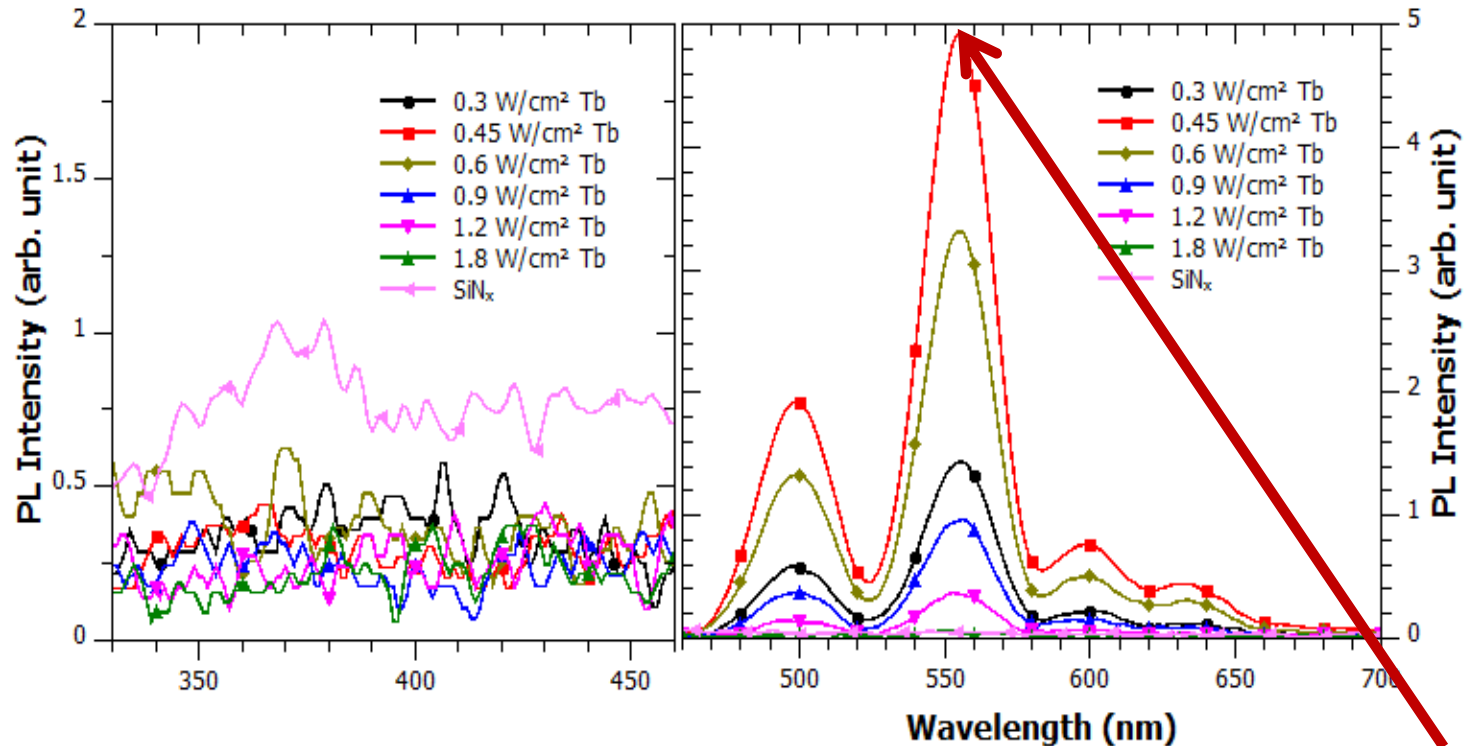


Matrix Emission around 400nm
→ fit with Tb³⁺ absorption by level 5D_4



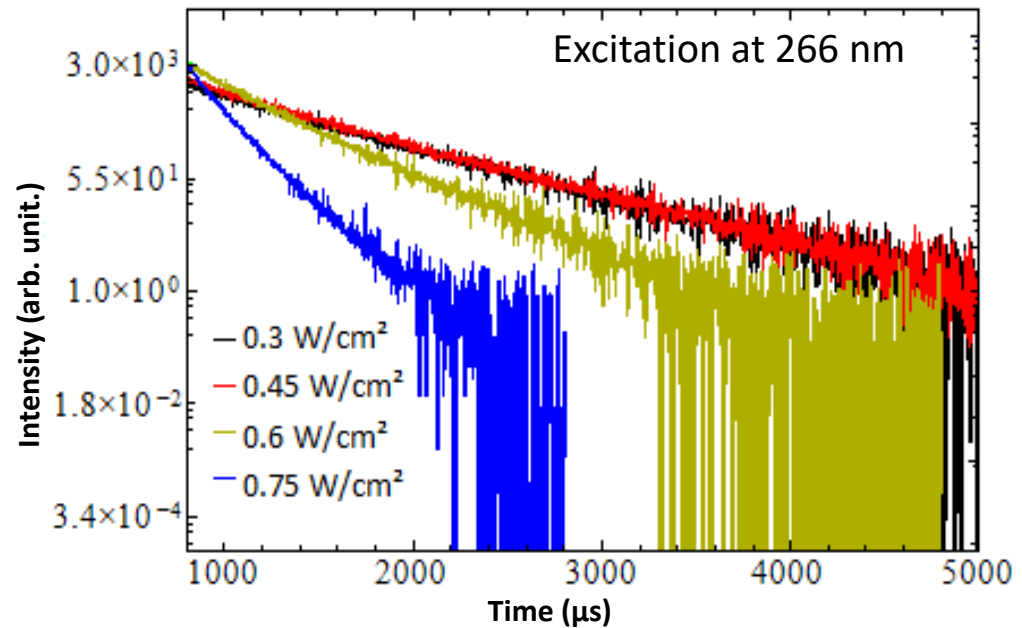
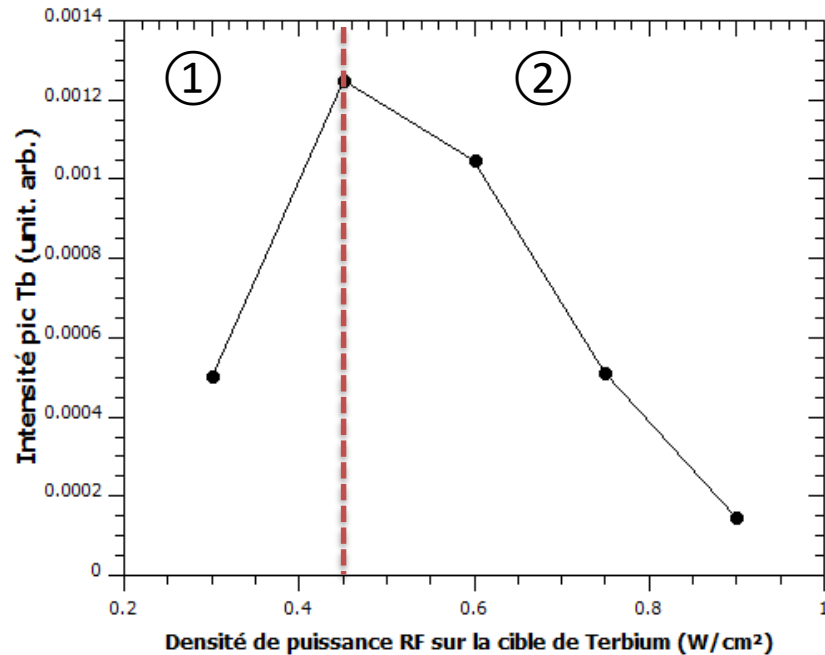
energy transfer may occurs

Energy transfer to Tb³⁺



- Extinction of SiN_x matrix luminescence
 - Increase of Tb³⁺ luminescence with Tb content
- Indirect excitation of Tb³⁺ ions
- Energy transfer (ET) from matrix to Tb³⁺ ions

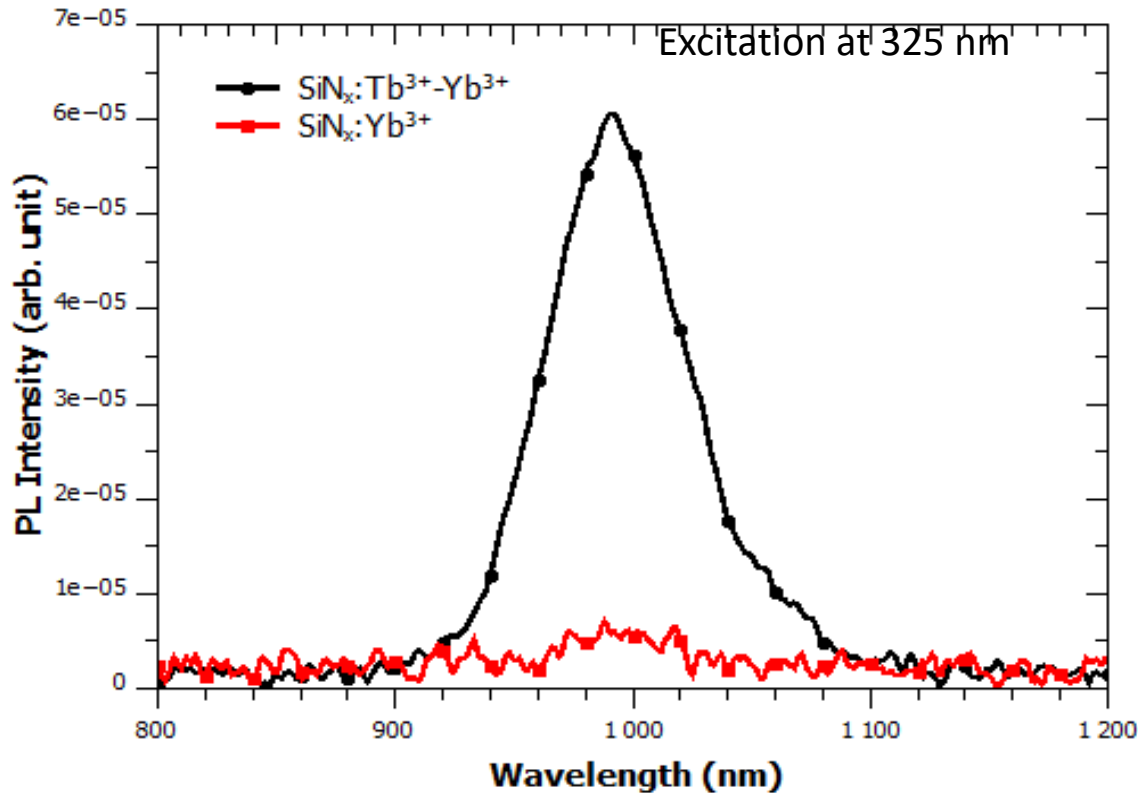
Tb³⁺ concentration effect on luminescence



- Extinction of Tb³⁺ luminescence and Tb³⁺ lifetime decrease with [Tb] increase

→ Concentration quenching

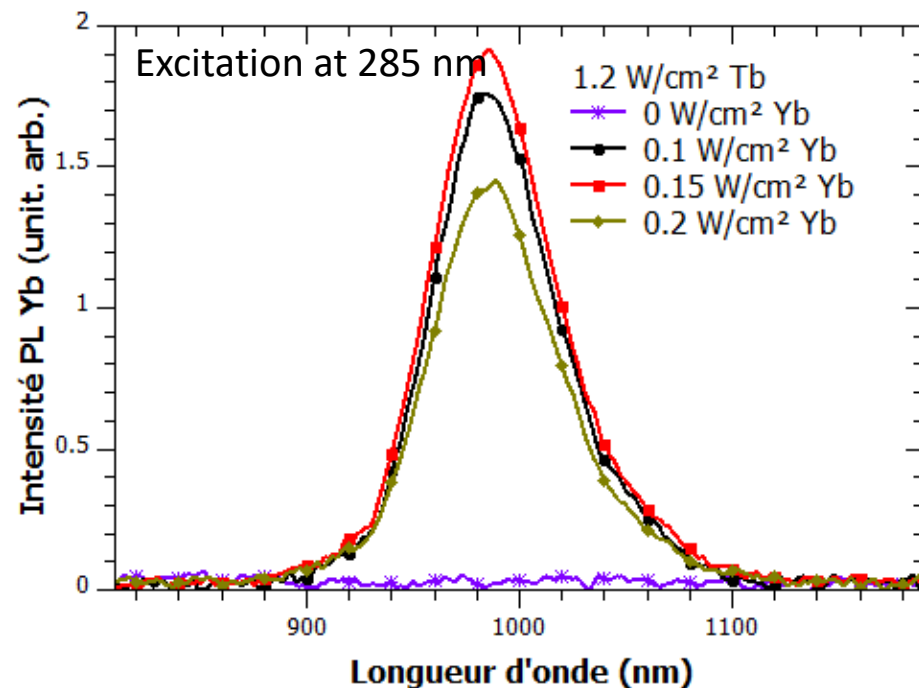
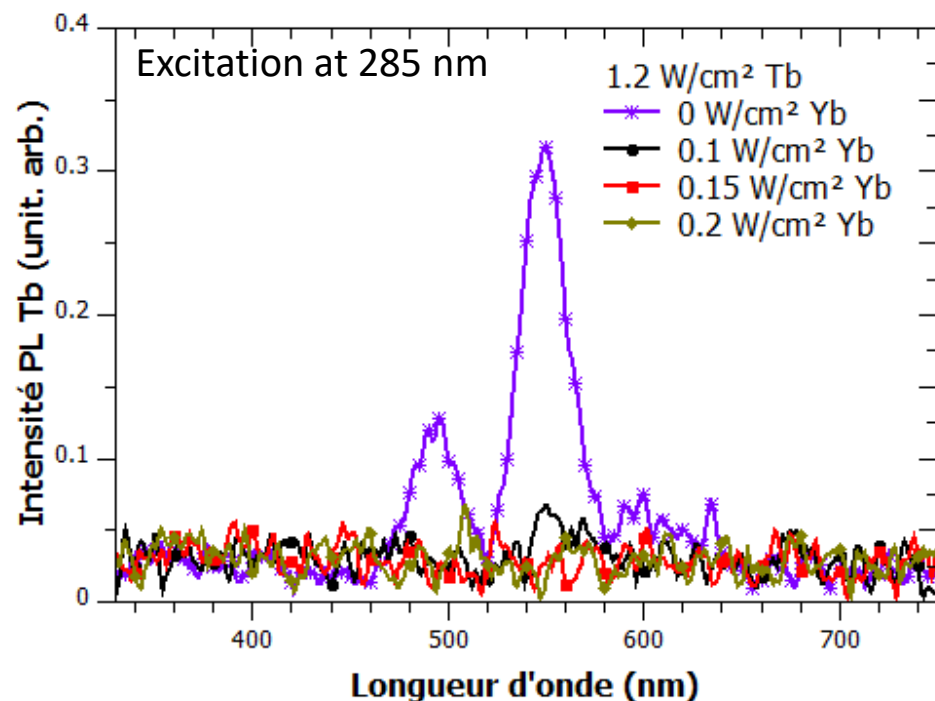
Energy transfer to Yb³⁺



- Yb³⁺ PL Intensity appears in the presence of Tb³⁺ ions
- Non-resonant excitation of Yb³⁺

→ Cooperative Energy transfer (CET) between Tb³⁺ and Yb³⁺ ions

Energy transfer from Tb³⁺ to Yb³⁺



- Tb³⁺ PL Intensity decrease with increasing Yb³⁺ content
- Yb³⁺ PL Intensity increase with increasing concentration
- Non-resonant excitation of Yb³⁺

→ Cooperative Energy transfer (CET) between Tb³⁺ and Yb³⁺ ions

SiN_x:Tb³⁺Yb³⁺

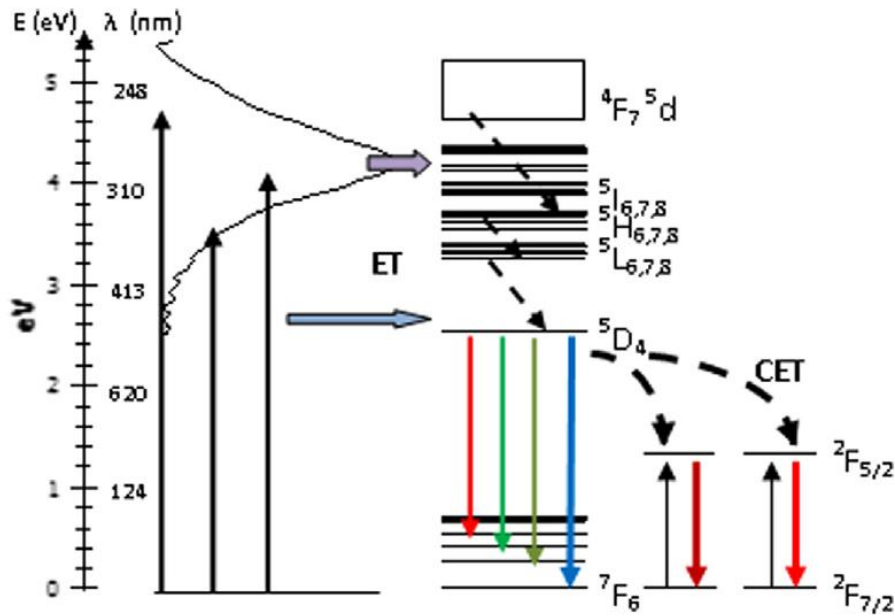


Fig. 5. Down-conversion process. A schematic of the energy levels of the down-conversion system with the excitation in black arrows, the radiative de-excitation (photon emission) in colored arrows, the non-radiative de-excitation in black straight dashed line arrows, the energy transfer in big blue arrows, and the cooperative energy transfer in black curved dash line arrows. (For interpretation of the references to color in this figure legend, the reader is referred to the web version of this article)

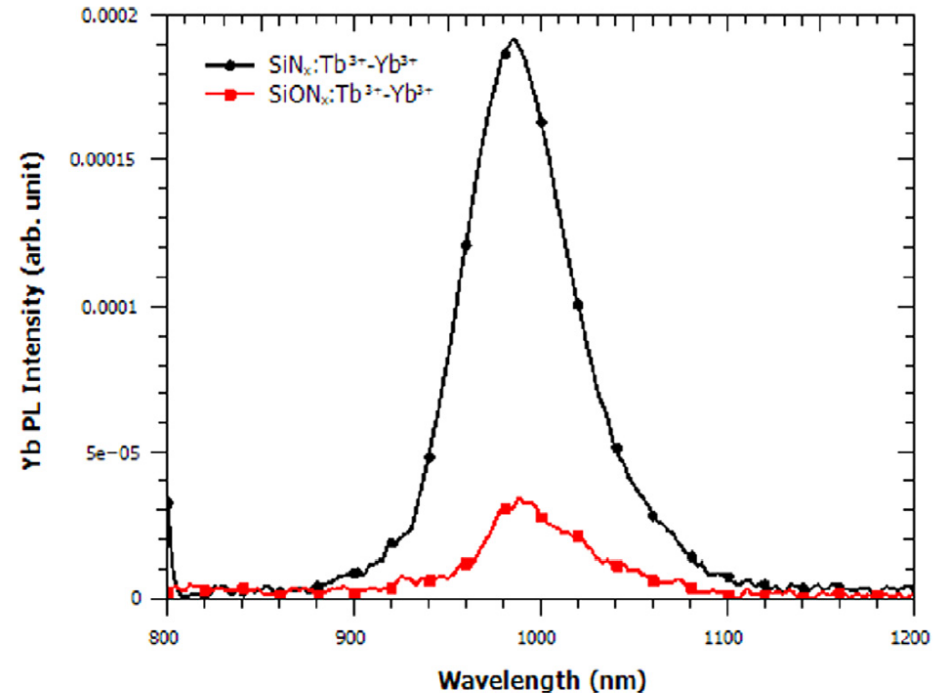


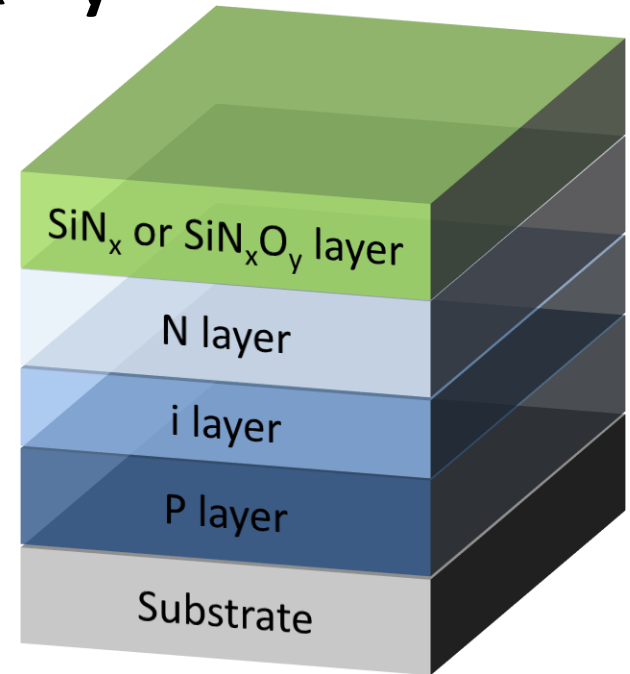
Fig. 9. Yb³⁺ emission for different matrixes. Photoluminescence spectra of the best samples obtained of SiN_x and SiO_xN_y co-doped matrixes for an excitation wavelength of 285 nm measured with a grating of 600 s/mm-750 bw.

SiN_x:Tb³⁺,Yb³⁺ versus SiN_xO_y:Tb³⁺,Yb³⁺

Table 1

Extraction efficiencies. Extraction efficiencies of the SiN_x and SiO_xN_y matrixes in the air, the layer, and the silicon.

η^{ext} (%)	Air	Layer	Silicon
SiN _x	15.8	60.8	23.4
SiN _x O _y	22.8	59.7	17.5



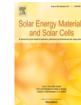
- **Internal efficiency of SiN_x based film is about 29 times larger than the one obtained with SiN_xO_y based film**
- **External efficiency of SiN_x based film (with extraction into the Si solar cell) is about 12 times larger than the one obtained with SiN_xO_y based film**
 - *Highly Efficient Infrared Quantum Cutting in Tb³⁺-Yb³⁺ Codoped Silicon Oxynitride for Solar Cell Applications, YT An et al, Advanced Optical Materials 1 (11), 855-862, 2013*
 - *SiN_x:Tb³⁺-Yb³⁺, an efficient down-conversion layer compatible with a silicon solar cell process, L Dumont et al, Solar Energy Materials and Solar Cells, 2016*

Down shifting layer



Solar Energy Materials and Solar Cells

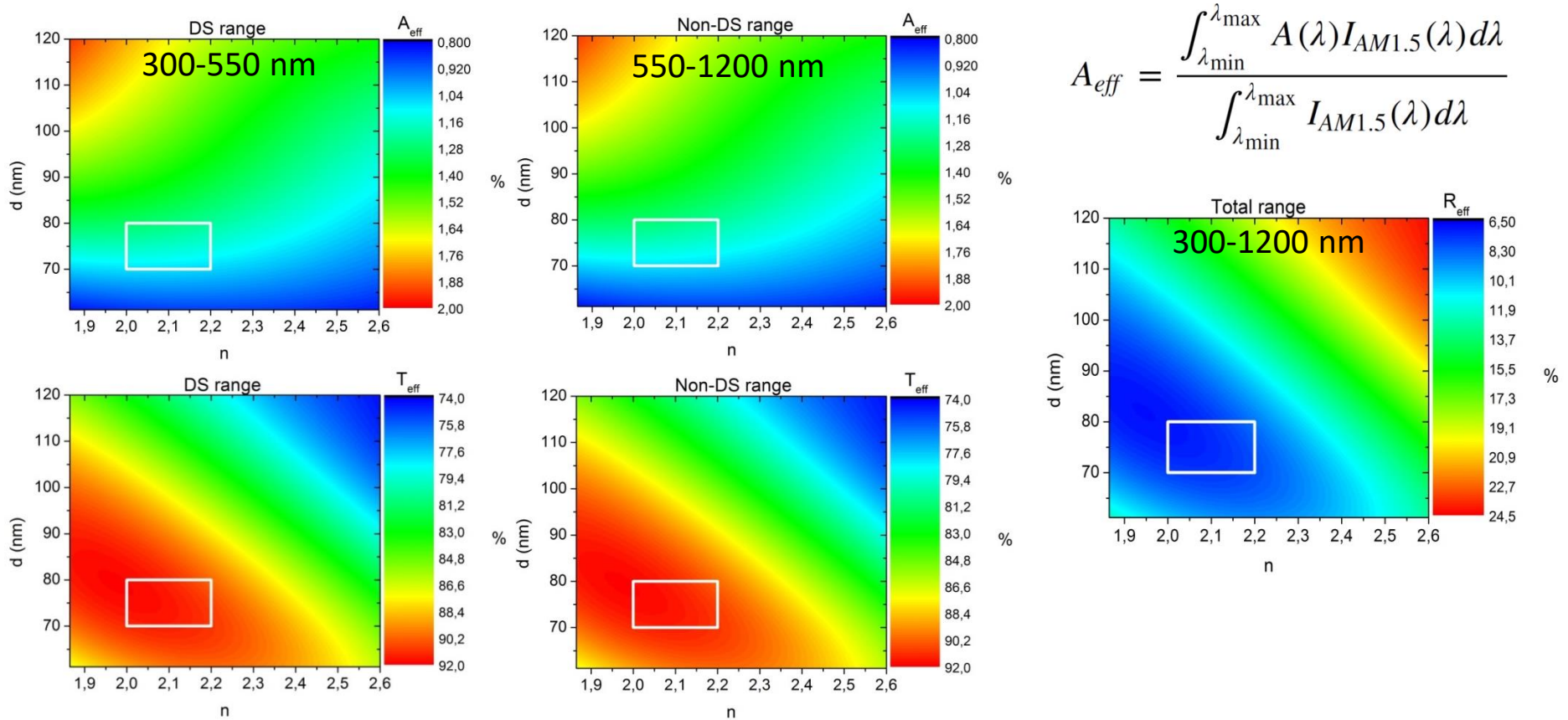
Volume 169, September 2017, Pages 132-144



Down-shifting Si-based layer for Si solar applications

L. Dumont ^a, P. Benzo ^{a, 1}, J. Cardin ^a, I.-S. Yu ^b, C. Labbé ^a, P. Marie ^a, C. Dufour ^a, G. Zatyb ^c, A. Podhorodecki ^c, F. Gourbilleau ^a

DS layer optical properties preliminary studies



$$A_{eff} = \frac{\int_{\lambda_{min}}^{\lambda_{max}} A(\lambda) I_{AM1.5}(\lambda) d\lambda}{\int_{\lambda_{min}}^{\lambda_{max}} I_{AM1.5}(\lambda) d\lambda}$$

- A_{eff} and T_{eff}
 \rightarrow compromise under $n=2,2$ and 100 nm

- R_{eff}
 $\rightarrow 2,0 < n < 2,2$
 $\rightarrow 70 \text{ nm} < d < 80 \text{ nm}$

PL Extraction efficiency $\text{SiN}_x:\text{Tb}^{3+}$

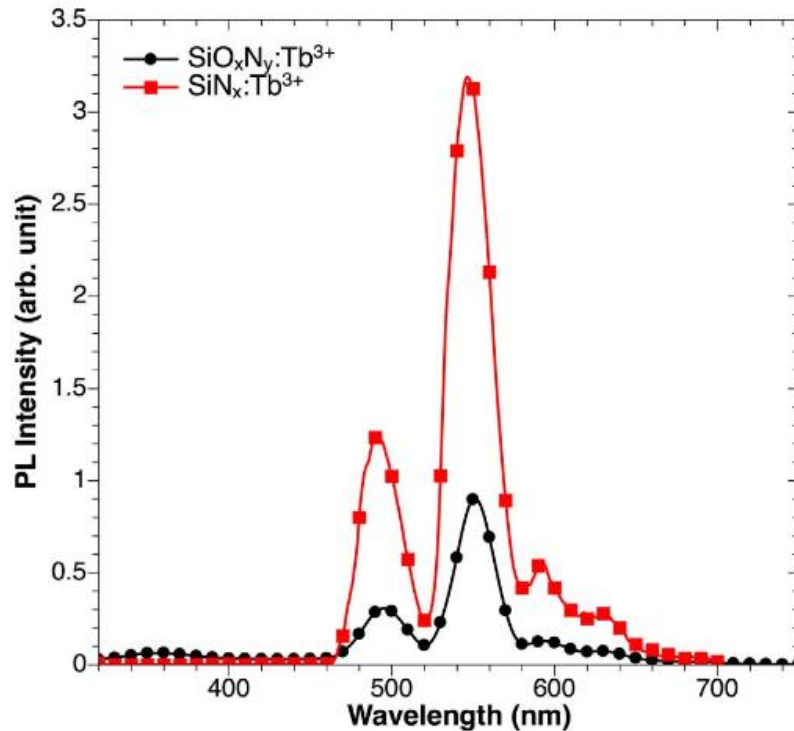


Fig. 15. Photoluminescence spectra of the optimized samples obtained of Tb^{3+} -doped SiO_xN_y and SiN_x doped terbium matrices for a 285 nm excitation wavelength measured with the 600 lines/mm-750 bw grating.

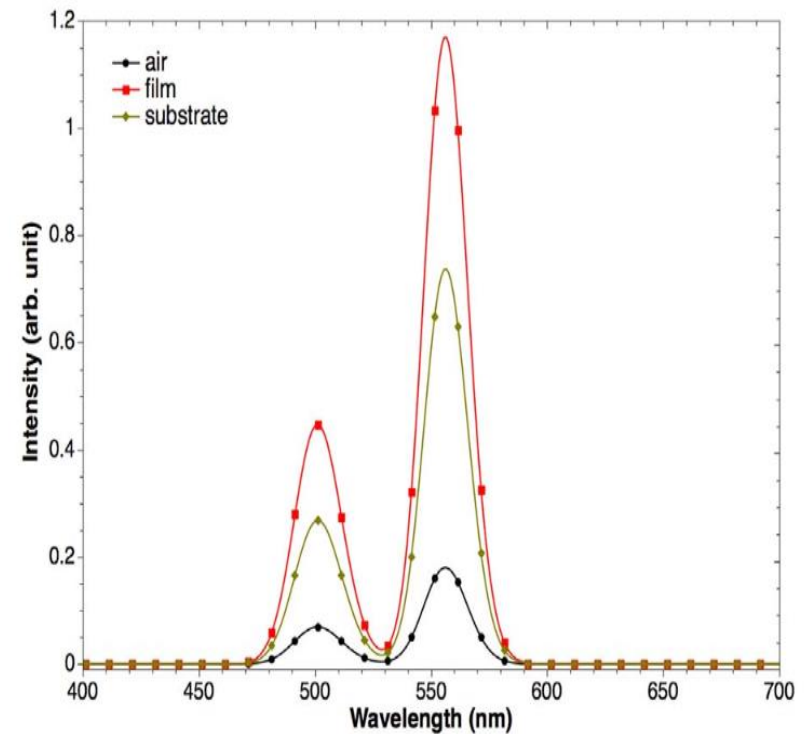


Fig. 1. Modeled Tb^{3+} PL spectra recorded in the three media, only the two more intense peaks/bands representing the 5D_4 to 7F_6 and 5D_4 to 7F_5 energy transitions are considered.

Table 2

Integrated luminescence efficiencies of the SiN_x and SiO_xN_y matrixes in the air, the layer, and the silicon.

η^{lum} (%)	Air	Layer	Silicon
SiN_x	8.7	56.3	35
SiN_xO_y	13.8	60.2	26

Larger efficiency of the DS layer with the SiN_x matrix than with SiN_xO_y due to larger Tb content and to larger extraction into the Si PV cell

- Down-shifting Si-based layer for Si solar applications, L Dumont et al, Solar Energy Materials and Solar Cells 169, 132–144, 2017

Integration in an industrial process

Received: 13 April 2018 | Revised: 6 July 2018 | Accepted: 30 July 2018
DOI: 10.1002/pip.3071

RESEARCH ARTICLE

WILEY **PROGRESS IN PHOTOVOLTAICS**



Journal of Rare Earths

Available online 7 November 2018

In Press, Accepted Manuscript ?

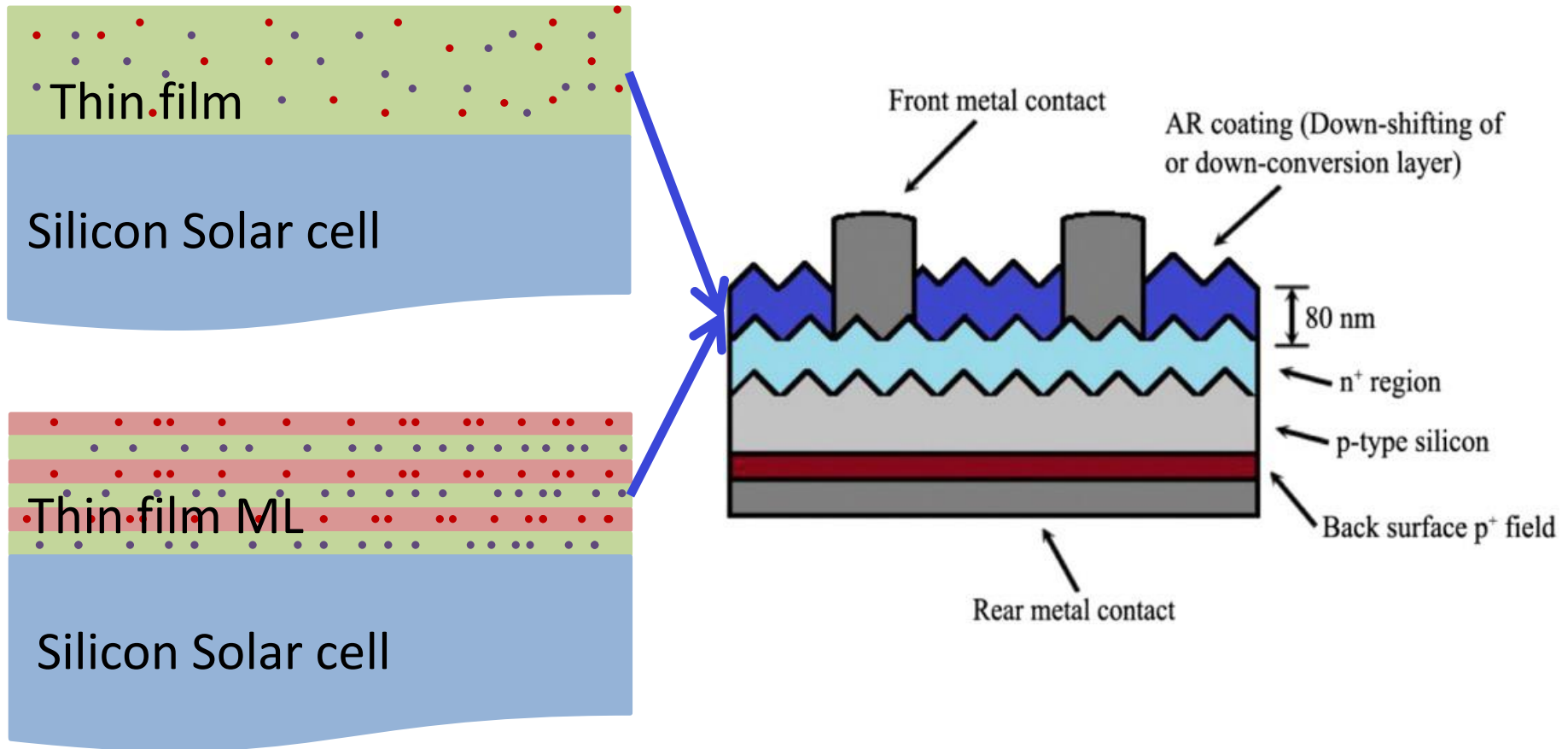


First down converter multilayers integration in an industrial Si solar cell process

Lucile Dumont¹ | Julien Cardin¹ | Christophe Labbé¹ | Cédric Frilay¹ |
Pierre-Matthieu Anglade¹ | Ing-Song Yu² | Maxime Vallet³ | Patrick Benzo³ |
Marzia Carrada³ | Didier Stiévenard⁴ | Hocine Merabet⁵ | Fabrice Gourbilleau¹

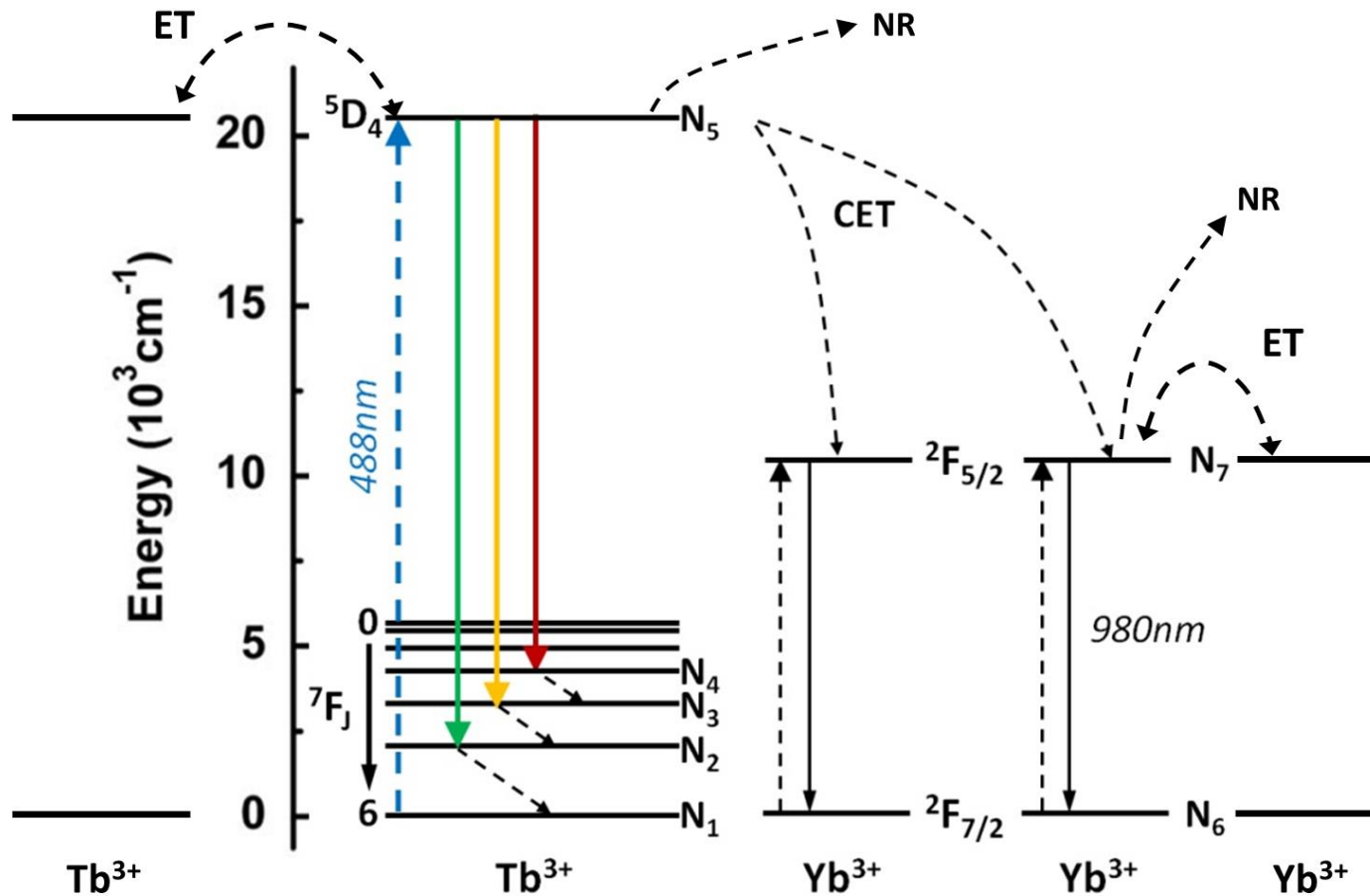
Monolithic crystalline silicon solar cells with SiN_x layers doped with Tb³⁺ and Yb³⁺ rare-earth ions ☆

Integration in an industrial process



Modeling of Donor (Tb^{3+})- Acceptor(Yb^{3+}) ions system

Modeling of Donor(Tb^{3+})-Acceptor(Yb^{3+}) ions system



Donor(Tb^{3+})-Acceptor(Yb^{3+}) ions system

Rate equations modeling of steady state of electronic energy levels

$$\frac{dN_1}{dt} = -\sigma\phi(N_1 - N_5) + \frac{N_5}{\tau_{51}^r} + \frac{N_2}{\tau_{21}^{nr}} + K_{CET}N_5N_6^2 + \frac{N_5}{\tau_{51}^{nr}} + k_{ET}(Tb^{3+})N_5$$

$$\frac{dN_2}{dt} = \frac{N_5}{\tau_{52}^r} + \frac{N_3}{\tau_{32}^{nr}} - \frac{N_2}{\tau_{21}^{nr}}$$

$$\frac{dN_3}{dt} = \frac{N_5}{\tau_{53}^r} + \frac{N_4}{\tau_{43}^{nr}} - \frac{N_3}{\tau_{32}^{nr}}$$

$$\frac{dN_4}{dt} = \frac{N_5}{\tau_{54}^r} - \frac{N_4}{\tau_{43}^{nr}}$$

$$\frac{dN_5}{dt} = \sigma\phi(N_1 - N_5) - \sum_{j=1}^4 \frac{N_5}{\tau_{5j}^r} - K_{CET}N_5N_6^2 - \frac{N_5}{\tau_{51}^{nr}} - k_{ET}(Tb^{3+})N_5$$

$$\frac{dN_6}{dt} = -2K_{CET}N_5N_6^2 + \frac{N_7}{\tau_{76}^r} + \frac{N_7}{\tau_{76}^{nr}} + k_{ET}(Yb^{3+})N_7$$

$$\frac{dN_7}{dt} = 2K_{CET}N_5N_6^2 - \frac{N_7}{\tau_{76}^r} - \frac{N_7}{\tau_{76}^{nr}} - k_{ET}(Yb^{3+})N_7$$

Cooperative energy transfer between Tb³⁺ Yb³⁺ ions

Energy transfer between Tb³⁺ ions (cross-relaxation)

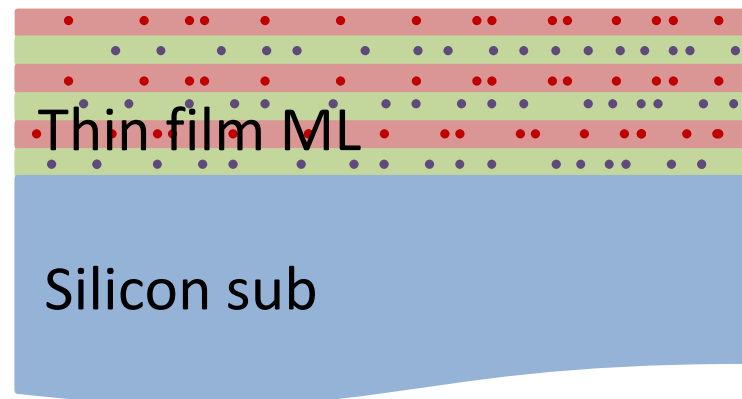
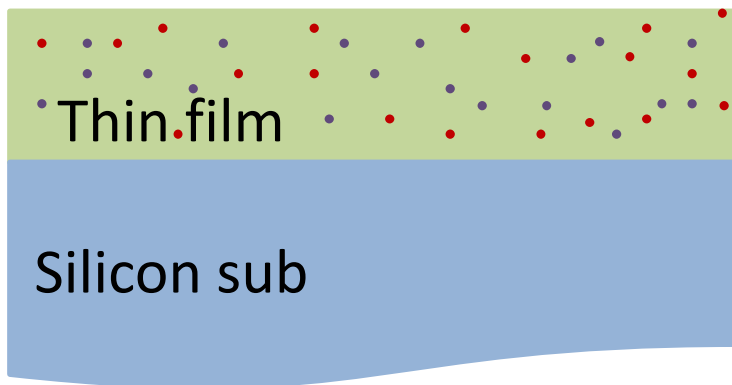
energy transfer between Yb³⁺ ions (cross-relaxation)

Look on modelling parameters

- K_{CET} , $K_{ET}(Tb^{3+})$ and $K_{ET}(Yb^{3+})$ distance dependent (r) and therefore function of concentration $[Tb^{3+}]$ and $[Yb^{3+}]$

$$K_{CET} \propto \frac{1}{r_{Tb^{3+}-Yb^{3+}}^6 \cdot r'_{Tb^{3+}-Yb^{3+}}{}^6} \quad K_{ET}(RE^{3+}) \propto \frac{1}{r_{RE^{3+}-RE^{3+}}^6}$$

- Those parameters are depending on statistical distribution of rare earth ion in thin films



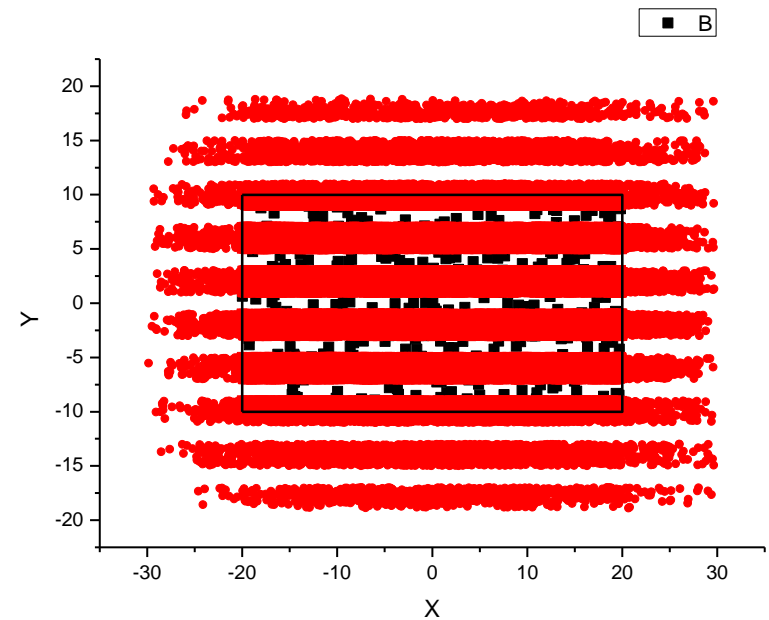
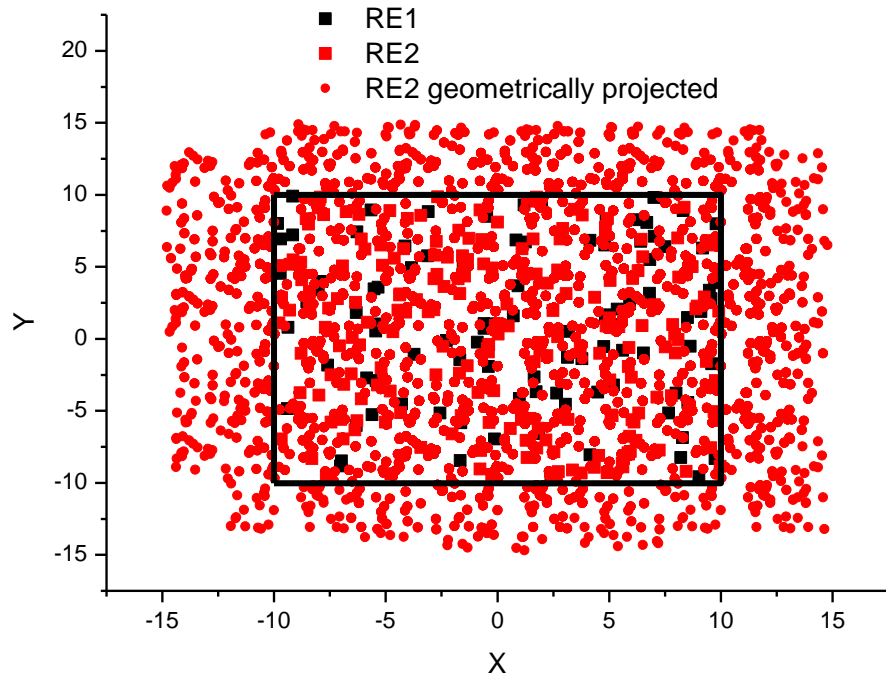
- Homogenous thin film and ML thin film allow to reach different kind of spatial distribution and concentration of rare earths ions

$$[RE^{3+}] \leq 10^{+20} \text{ cm}^{-3}$$

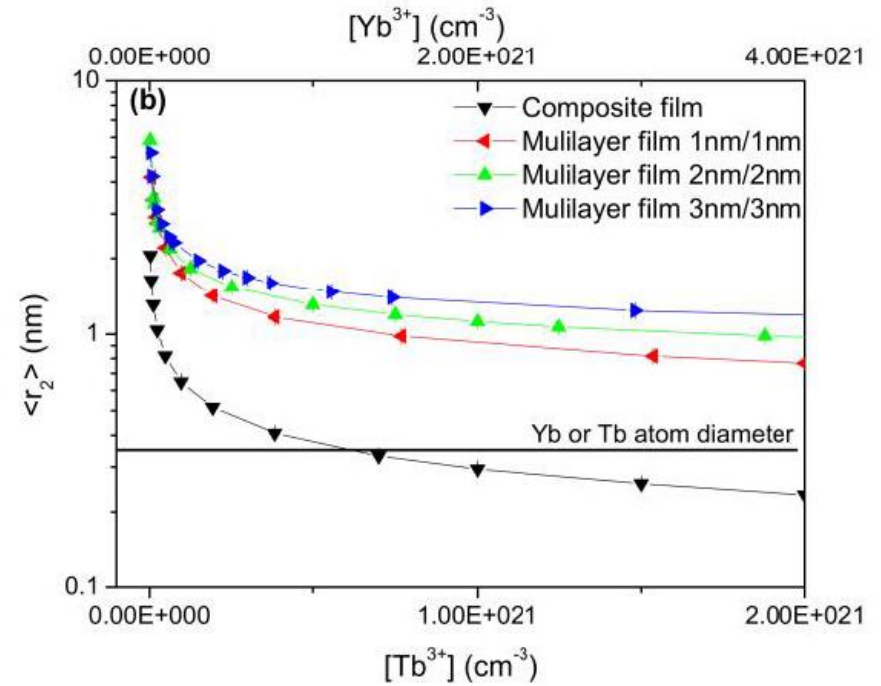
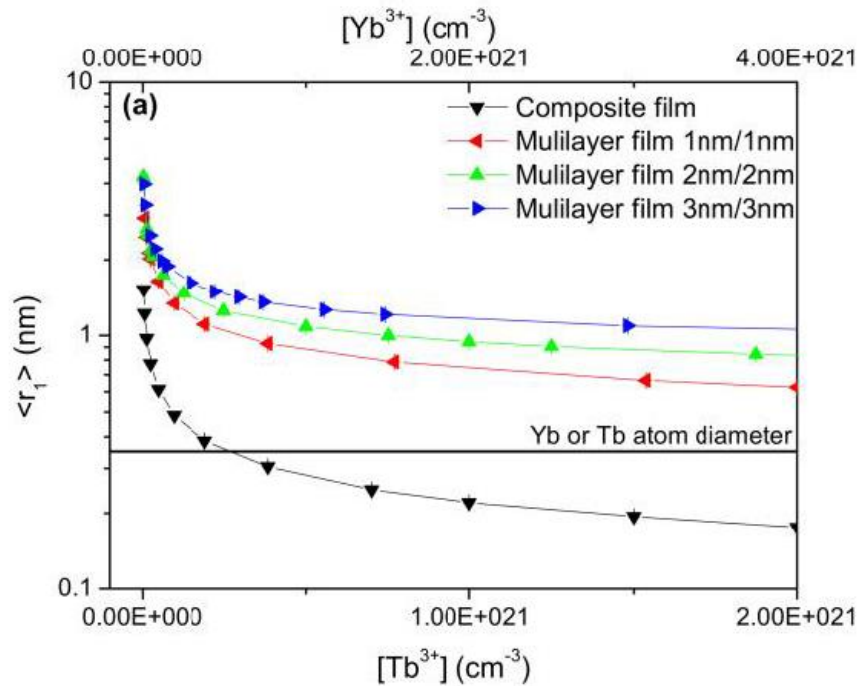
$$[RE^{3+}] \leq 10^{+21-22} \text{ cm}^{-3}$$

Comparison of homogenous thin film and multilayer systems

- Monte Carlo method for determination of average distance between first, second...neighbors



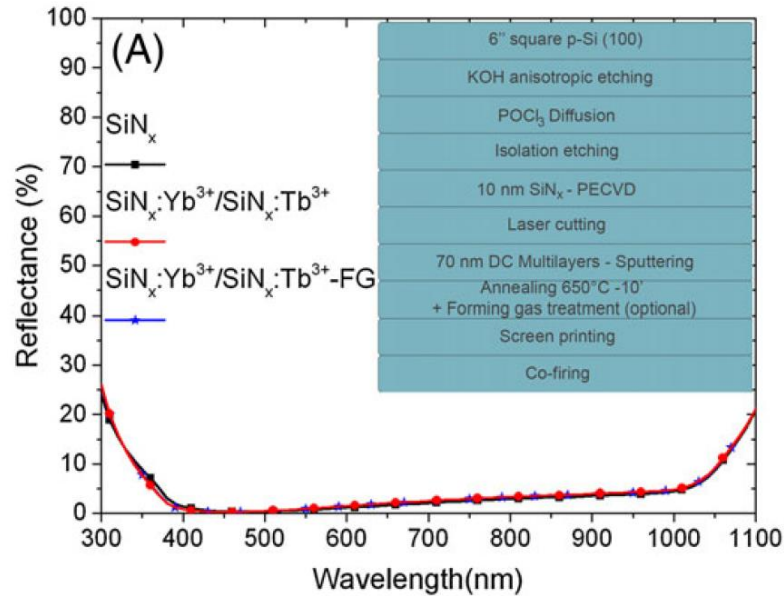
Thin film and multilayer systems



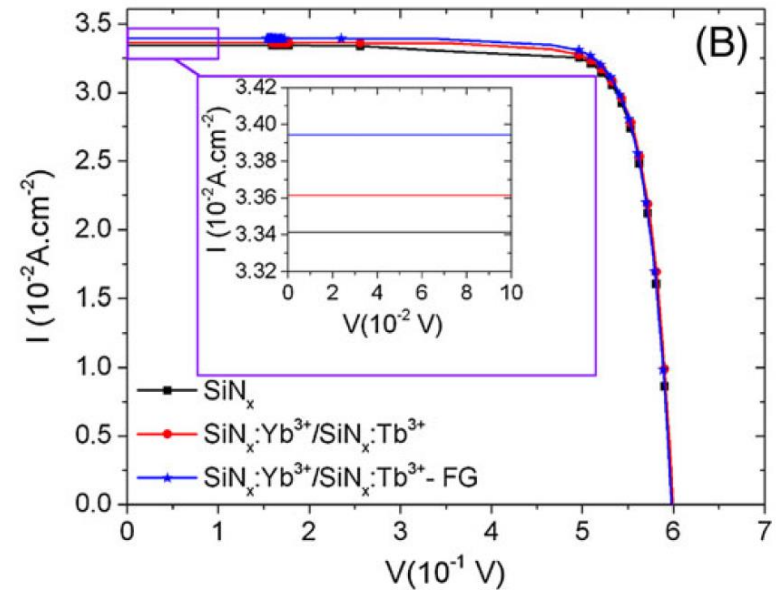
→ ML prevent aggregation quenching and allow therefore higher doping rate

Integration in an industrial process

Multilayer Integration on silicon solar cell



Reflectance of three layers (SiN_x, SiN_x:Yb³⁺/SiN_x:Tb³⁺ MLs, SiN_x:Yb³⁺/SiN_x:Tb³⁺ MLs with forming gas post treatment) deposited on textured emitters.



I-V curves corrected of series resistance for three c-Si solar cells topped with SiN_x, SiN_x:Yb³⁺/SiN_x:Tb³⁺ MLs and SiN_x:Yb³⁺/SiN_x:Tb³⁺ MLs with forming gas post treatment

ARC Layer	V _{OC} , V	J _{SC} , mA·cm ⁻²	Pseudo FF	Pseudo Efficiency (%) ± 0.03%
SiN _x	0.605	33.41	0.82	16.48
XC25(1.5/1.5)	0.599	33.61	0.82	16.53
XC25(1.5/1.5) + FG	0.598	33.94	0.82	16.66

Established Improvement of solar cell efficiency



Monolayer Integration on silicon solar cell

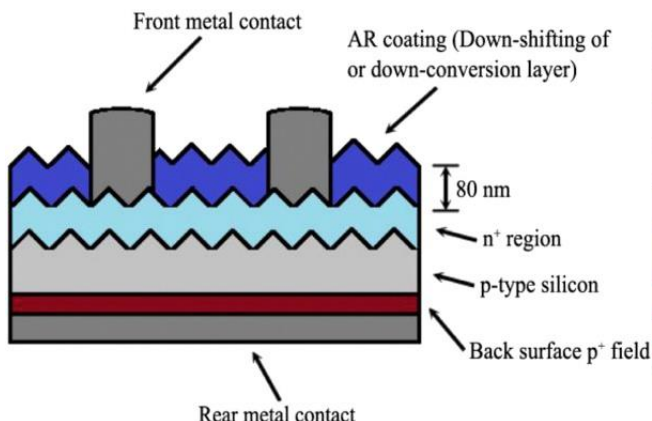
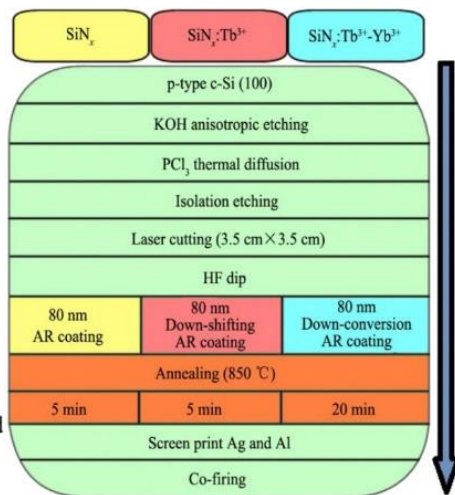
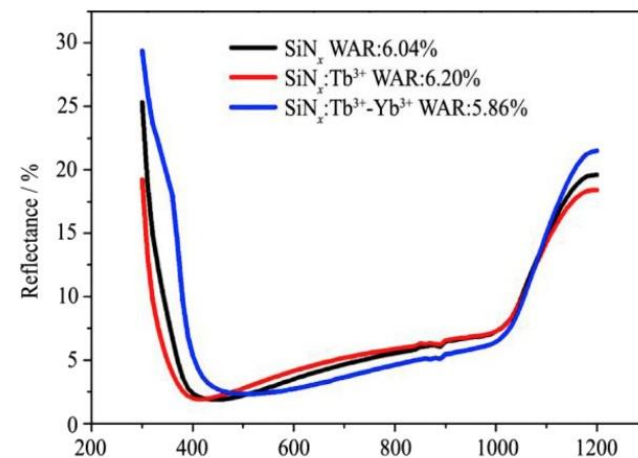


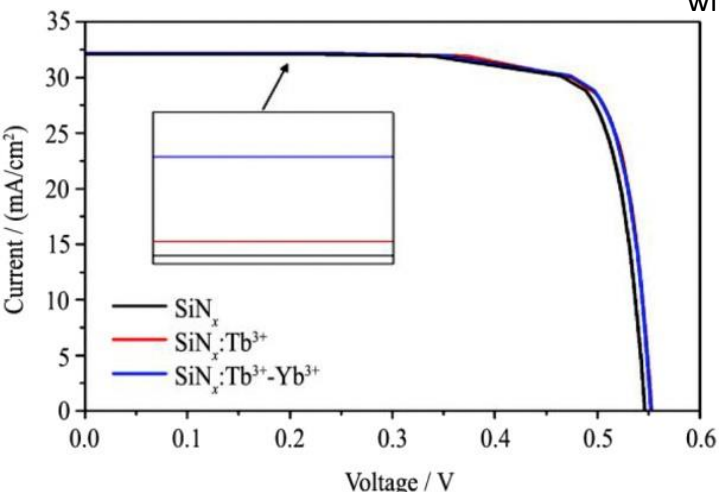
Diagram of c-Si solar cells with spectrum conversion layers



Process flow of c-Si solar cells with spectrum conversion layers.



Reflectance of three layers deposited on textured emitters



Pseudo *I-V* curves for three c-Si solar cells with SiN_x , $\text{SiN}_x:\text{Tb}^{3+}$ and $\text{SiN}_x:\text{Tb}^{3+}-\text{Yb}^{3+}$ layers, respectively.

Samples	J_{sc} (mA/cm ²)	V_{oc} (V)	Pseudo FF (%)	Pseudo Efficiency (%)	Efficiency to normalized transmission (%)
SiN_x	32.091	0.546	0.804	17.13	18.23
$\text{SiN}_x:\text{Tb}^{3+}$	32.098	0.552	0.803	17.31	18.45
$\text{SiN}_x:\text{Tb}^{3+}-\text{Yb}^{3+}$	32.165	0.552	0.806	17.36	18.44

PV performances of c-Si solar cells with SiN_x , $\text{SiN}_x:\text{Tb}^{3+}$ and $\text{SiN}_x:\text{Tb}^{3+}-\text{Yb}^{3+}$ layers

relative increase by 1.34% in the conversion efficiency



Conclusion

- Established results:
 - SiN_xO_y and SiN_x based DC, DS layer
 - Integration of ML and homogenous DC layer in an industrial process of Si PV cell
 - **relative increase by 1.34% in the conversion efficiency**
- Perspectives:
 - Ce^{3+} emission in $\text{SiN}_x\text{O}_y/\text{SiN}_x$ layer ->increase of excitability
 - Distance distribution model in material -> further improvement
 - Up conversion layer with Er^{3+}

Acknowledgements

NIMPH Team (CIMAP):

L. Dumont, F. Ehré, Y.-T. An, J. Weimmerskirch-Aubatin, X. Portier, P. Marie, C. Dufour, F. Gourbilleau, C. Labbé

Colleagues:

J.-L. Doualan (FR), A. L. Richard(USA), D. C. Ingram(USA), C. Labrugère(FR), I. S. Yu(TW), A. Podhorodecki (PL), G. Zatoryb (PL), M. Carrada (FR), P. Benzo (FR), M. Vallet(FR), W. M. Jadwisieniczak(USA), H. Merabet(Qatar)



Partenariat Hubert Curien (PHC)
France-Taiwan ORCHID

**Collaboration with E-Ton Solar
(Taiwan)**

Thank you